Design of an Endoscopic Biopsy Needle with Flexural Members

By

Stacy L. Figueredo

SUBMITTED TO THE DEPARTMENT OF MECHANICAL ENGINEERING IN PARTIAL FULFILLMENT OF THE REQUIREMENTS FOR THE DEGREE OF

MASTER OF SCIENCE IN MECHANICAL ENGINEERING
AT THE
MASSACHUSETTS INSTITUTE OF TECHNOLOGY

SEPTEMBER 2006

Signature of Author:

Department of Mechanical Engineering
August 18, 2006

Certified by:

Alexander H. Slocum
Professor of Mechanical Engineering
Thesis Supervisor

Accepted by:

Lallit Anand
Professor of Mechanical Engineering
Chairman, Department Committee on Graduate Students

Design of an Endoscopic Biopsy Needle with Flexural Members

by

Stacy L. Figueredo

Submitted to the Department of Mechanical Engineering
on August 18, 2006 in Partial Fulfillment of the
Requirements for the Degree of Master of Science
at the Massachusetts Institute of Technology

ABSTRACT

As a minimally invasive means of extracting a tissue sample from a patient, current endoscopic biopsy needles generally do not preserve tissue histology and often require multiple attempts to obtain a tissue sample. This paper presents an endoscopic biopsy needle with internal flexures that enable tissue to enter the hollow needle and then be severed from surrounding tissue when the needle is withdrawn. Using force-deflection and sample weight data from 10x scaled prototypes, variations of a flexural design captured 1.1 grams of a tissue phantom on average, as compared to wedge-type designs that averaged of 0.7-0.8 grams. Peak entrance forces for the flexure design were lower than for both wedge and extended wedge designs, and resistance forces were higher upon needle extraction. A low-angle 15-degree feature produced lower entrance resistance and larger exit resistance compared with 30 degree, 45 degree, and 60 degree features, which is desirable when retaining tissue. Manufacturing of a 1x scale prototypes, using a grinding and laser cutting process, suggested that flexural features could be produced in current endoscopic biopsy needles, but changes to the beveled cutting tip would first have to be made before flexural elements could be tested on actual liver samples.

Thesis Supervisor:
Professor Alexander H. Slocum
Department of Mechanical Engineering

Table of Contents

List of Figures

List of Tables

Acknowledgements

Margo Figueredo is not here today to read this paper. She died in April of 2005 of pancreatic cancer, after smiling and cheering everyone up about her own illness. My aunt was one of my biggest supporters throughout my years MIT and she was one of the few people who would understand how this project helped me to not feel so helpless about her being gone. I hope that, in some form, the work in this paper can help others who are going through a similar struggle as hers.

I would like to thank Professor Alex Slocum for being an advisor that will help with the fun parts of a project and the frustrating parts. His graduate class, 2.75 Precision Machine Design, was where I was first presented the problem of working on an improved endoscopic biopsy needle, and where I first started working with other students on a possible solution. Ever optimistic, always realistic. Thanks so much for your advice.

Another close advisor for this Project was Dr. William Brugge of Massachusetts General Hospital, who volunteered many hours of his time to giving me advice and design ideas for the project. As an expert in the fields of gastroenterology and endoscopy, Dr. Brugge's expertise was critical to understanding the problem and scope of the project.

Initial research on the endoscopic biopsy needle design was conducted with a great team of students during the MIT course 2.75 Precision Machine Design: Andrew Carvey, Bill Fienup, Barry Kudrowitz, and Jacob Wronksi. Maureen Lynch, our administrative assistant who keeps this side of the building from collapsing under a pile of paper, was always around to help. I appreciate the help of Professor Mary Boyce and Asha Balakrishnan for frequent use of their lab and assistance with the TA.XT setup and Massachusetts General Hospital for use of their facilities and excellent staff. Vendors in

the medical industry are mentioned throughout the paper that were particularly helpful during this project and should be recognized for their excellent service.

Of course, this project could not have been completed without the financial support and technical experience of The Center for Integration of Medicine and Innovative Technology (www.cimit.org). CIMIT has supported this project with funding provided from the U.S. Army Medical Acquisition Activity (USAMRAA) under cooperative agreement no. DAMD 17-02-2-0006. The content of this information does not necessarily reflect the position or policy of the Government, and no official endorsement should be inferred. (Although I hope they like it.)

Chapter 1

INTRODUCTION

Gastrointestinal (GI) cancers are the most common malignancy in the United States, and cancer of the gastroesophageal junction is the most rapidly increasing cancer in the US.[1] The vast majority of GI cancers are diagnosed with endoscopic instruments that travel through the esophagus to obtain high resolution video and ultrasound images. Along with ultrasound imaging techniques, tissue-sampling procedures, known as biopsies, provide vital information about abnormal cellular development and tissue composition. According to a National Health Statistics study taken in 1996, over 1.2 million endoscopic biopsies are performed in the United States each year[2]. Even with this level of testing, the 5-year survival rates for gastrointestinal cancers remains relatively low. The five-year survival rate for a tumor less than 2cm and confined to the head of the pancreas at the time of resection is approximately 20%.[3]

With most forms of cancer, an early and accurate diagnosis is critical for improving survival statistics. In the case of gastrointestinal cancers, endoscopic tissue biopsy is a key tool for early determination of the histological and cytological makeup of a lesion or grown. Current endoscopic biopsy designs may use a forceps mechanism or a hollow coring needle to obtain a tissue sample from a suspicious growth. These devices range in size from 14-gauge to 23-gauge hollow needles and larger scoop-shapes, but for GI

procedures, all must be deployed through the small inner channel of an endoscope. Both of these current designs often require multiple attempts to acquire samples for cytological and histological analysis of tissues. This can be because the sample is not large enough (either as a mass measurement or in length), or because the tissue organization has been damaged during retrieval. In either case, such a result may delay or prohibit proper diagnosis.

This inability to reliably obtain a tissue presents the problem with current endoscopic biopsy tools and with biopsy needles in particular. If a sample of tissue is not retrieved the first time a needle is inserted into a patient, the doctor may have to create additional tissue puncture sites, which introduces unnecessary patient trauma. Current endoscopic biopsy procedures also require sedation, which is in some way trauma to the patient on top of the wound created by tissue removal. If an adequate sample is not retrieved during the initial endoscopy procedure, anesthesia and additional procedures would be necessary. Of course, the financial costs of repeat procedures, more needles used, additional equipment time, and increased loading on staff, are absorbed by both hospitals and the patient. Given the improvements in care, accuracy in diagnosis, and cost savings that could be achieved by investigating biopsy needles, it was determined that an assessment of current technology and new design for clinical use would be worthwhile.

As described in detail, this project focuses on the development a safe and reliable endoscopic biopsy that improves tissue sampling success rates and preserves the histology of tissue samples. In order to increase the sampling output of a coring biopsy needle, researchers investigated several methods to improve the design. Active and passive methods of obtaining tissue samples were compared from both the end and the side of a cylindrical needle. After studying the overall means of sampling, methods of increasing shear force to overcome the force required to cut tissue were developed. A specific method for cutting and retaining tissue using a device with low entrance resistance but high exit resistance in order to cut and retain the tissue sample was

developed. Such a design allows tissue to enter the cavity of the needle when it is cut, but prevents the sample from exiting to such an extent that it is separated for the bulk of the suspect tissue and can removed from the body for testing purposes.

The final design employed a set of flexures that were angled into the needle. As this needle pierces tissue, its flexures open and allow a sample into the hollow needle tip. Upon extraction of the needle, forces normal to the needle axis cause the flexures to close, and shear forces sever the sample from surrounding tissue preserving a core sample inside the needle tip. This concept was tested using 10x scale stereolithographed needles and a gelatin tissue phantom to determine optimal feature dimensions. These results were used to prototype 1x scale 19-gauge stainless steel needle tips with laser cut features.

This paper presents the development of the aforementioned biopsy needle from functional requirements to final design. Included are an overview of existing technology, and the constraints of the biopsy procedure on a needle design, as well as the functional requirements and design parameters of the device. Early concept development, which was crucial in quickly pinpointing a solution, is presented, along with some of the basic mechanical principles underlying the flexural design. Finite element analysis of critical components is given where necessary to ensure soundness of the design, as well as some of the basic scaling that went into needle prototypes. Data from 10x needle tests of flexures compared to similar design features is presented as support for the flexural design over other geometries, as well as for determination of optimal parameters. Manufacturing and testing of 1x prototypes is given as an accurate assessment of the device design. A discussion of results presents needle performance as compared to the original device requirements. Finally, concluding remarks about future manufacturing possibilities and references to alternative materials are given.

Chapter 2

BACKGROUND

As with most precision devices, medical products in particular, a significant amount of background research must be conducted to understand an underlying problem that is not necessarily in a primary area of engineering. This allows an engineer to obtain enough information about an area to develop functional requirements for a device - measures of success that ensure desired results, which generally involves accurate and safe the implementation of the product. In order to develop an improved endoscopic biopsy tool, existing endoscopic biopsy needle designs and their capabilities are described in this section. The current endoscopic biopsy procedure is described to explore how this sequence of events may allow for design improvements. Ultrasound treatments are briefly described to introduce some design features that may be beneficial to needle tip visibility. Anatomical data for the gastrointestinal system, which affects needle dimensions and strength requirements, is also discussed. An overview of pathological tissue samples is given to understand why histological information is important to a sample, as well as how this diagnostic step affects device design. Finally, this background information is tabulated into the functional requirements for a proposed design.

2.1 Current Biopsy Needle Design Overview

Exactly how "the business end" of a needle obtains a sample though is relatively flexible from a design standpoint. To discover the design opportunities for such a device, we will see how a typical needle is designed, its major components, what the core purpose of these features are, and later, how such components can be redesigned to improve the reliability of an endoscopic needle biopsy.

The needle assembly has several components (see Figure 1). First, the sheath of the needle is a thin flexible plastic tube with a low coefficient of friction such that the long metal needle can slide inside it without sticking. The sheath serves a dual purpose of protecting the interior of the endoscope and preventing the needle from cutting into tissue before reaching the biopsy site. It would most likely be an extruded part during the manufacturing process due to its uniform cross-section and thin wall.

Along the inside of the sheath lies the actual coring needle, which is a hollow ultra-thin wall tube of 304 or 316L stainless steel. The needle is slightly longer than the endoscope (138mm to 140mm) and is sharpened to a beveled point. Typical medical bevels between 18 and 45 degrees exist depending on the application (tissue coring, fluid extraction, fluid injection, etc.). The needle gauge determines the outer diameter of the needle and may vary from a large 16-gauge needle to an extremely fine 23-gauge depending on the application. The wall thickness for any specific needle gauge outer diameter determines both the buckling strength of the needle as well as the maximum coring area, and is commercially available in wall thicknesses as thin as 0.0508mm (0.002in). Ultrasound features such as dimples or polymer coatings may be added to the needle tip as well, as explained in Section 2.3. This needle may perform the sampling operation using either a side cutting mechanism or the core of a hollow needle tip. Although, current models are exclusively made of stainless steel, some background

research has shown a potential for high flow length polymers in the production of needles.

Another feature of an endoscopic biopsy needle assembly is a removable stainless steel stylet that runs down the interior of the hollow needle. The stylet is a thin rod that prevents a needle from collecting tissue before reaching the desired sample site. By blocking the hollow inner needle channel and extending past the pointed needle with its beveled tip, the stylet ensures there is no unintended tissue puncture. It is also used to push tissue out of the needle once a sample has been gathered. This component can be seen in Figure 1.

A multifunctional handle is the final component in the needle assembly. Although dependent on the manufacturer, the controls typically work in such a way that the needle slides relative to the sheath. This handle is used by a doctor or technician to control the extension and location of the needle, as well as to provide the cutting action if passive or to trigger the device if active. A location to insert and remove the stylet is accessible from the handle area, and for aspiration needle, a syringe can be attached to provide suction. As an example, the handle of a Cook® endoscopic biopsy needle with the syringe attachment is shown in Figure 1b and Figure 1c.

Although improvements to all components ultimately provide the best overall improvements to the endoscopic biopsy needle design, the focus of the needle design for the purpose of this research will be the needle itself. This more than likely will affect the design of the control handle, sheath, and stylet, but is considered a secondary to the needle shape.

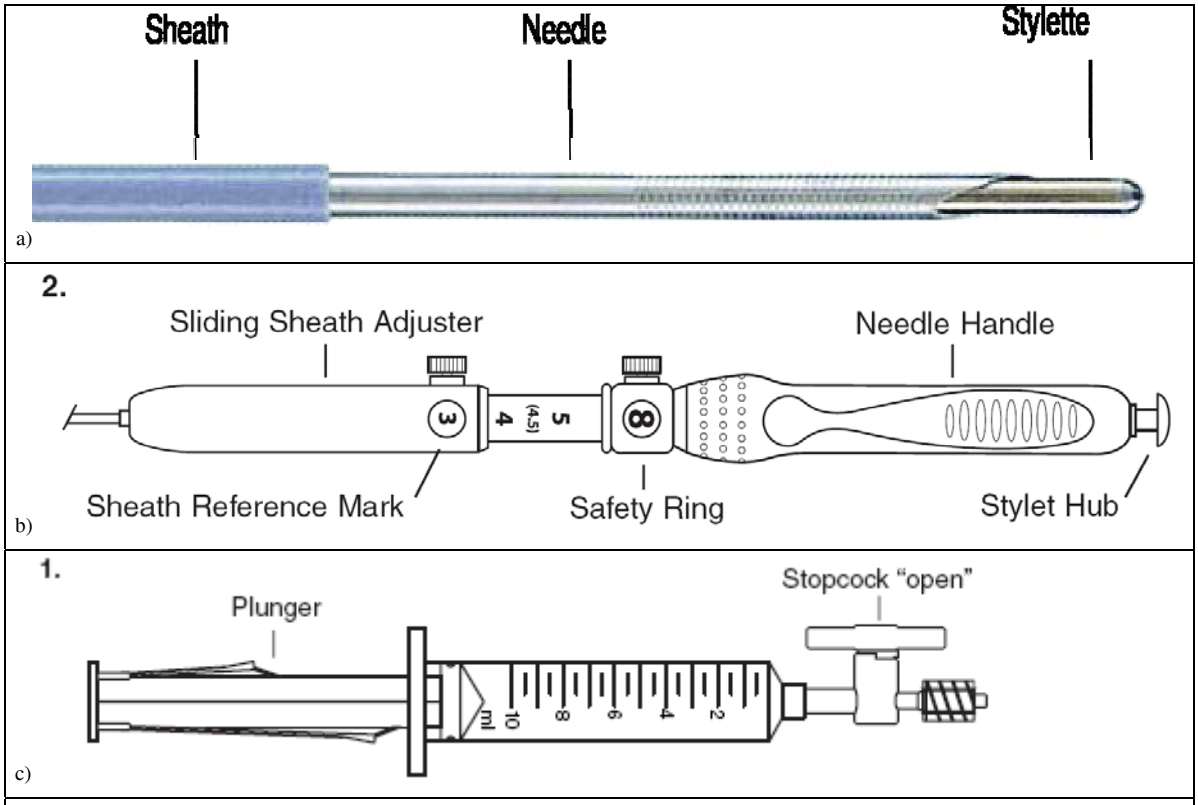

Figure 1: Echotip Ultra Ultrasound Needle and typical needle components labeled. Source: Cook Endoscopy

2.2 Endoscopic Procedure

Exactly how a biopsy needle travels to a lesion in the body is another important aspect of the design, which can be described by analyzing the endoscopic biopsy procedure (Figure 2). A typical endoscope can be thought of as a semi-flexible tube, with a control section that allows the doctor to bend the endoscope head (Figure 3). On the head of the endoscope are an ultrasound device, the opening of an air or liquid flushing channel, and the opening of the channel used for biopsy tools and other instruments (Figure 4). For the first step of an endoscopic biopsy, the endoscope is introduced through the mouth and is carefully guided via the esophagus, into the stomach, and then through the gastrointestinal system to the general area of the lesion using a small camera on the end of the tool (Figure 2). The flushing system clears the way for viewing the area and can prepare for the sampling step.

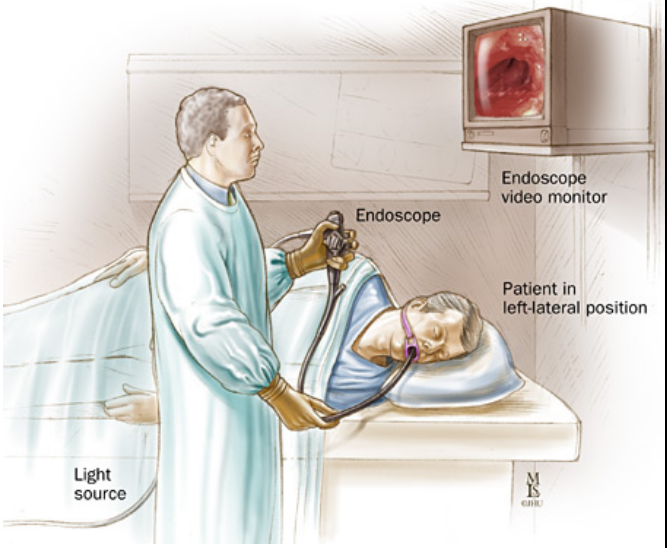

Figure 2: Room set-up and patient positioning for endoscope. Source: Johns Hopkins Medical Institutions Digestive Disease Library

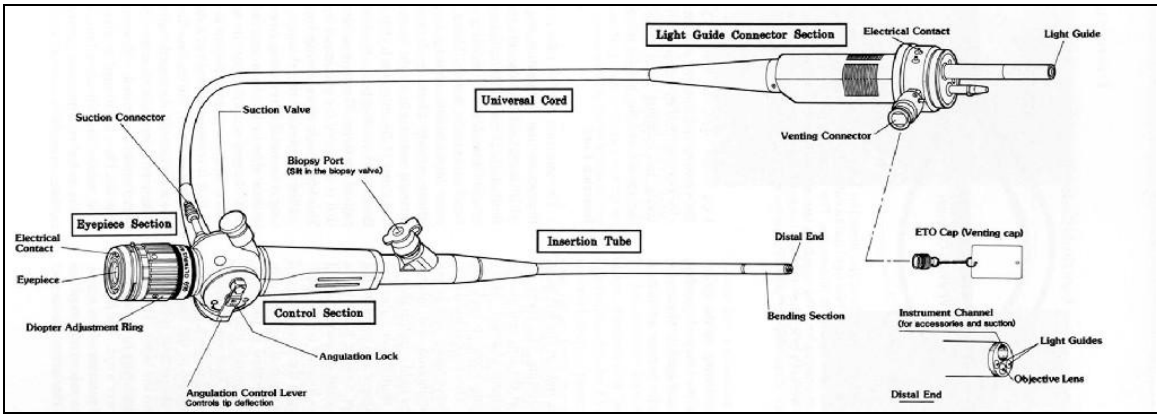

Figure 3: Typical components of an endoscope with components labeled. (Source: eyedesignbook.com)

During the next step of the procedure this ultrasound device is used to image the subsurface of the site and some of the organs that lie on the other side of the gastrointestinal wall, which helps to determine the exact site of a tumor or growth. After the endoscope is in place, a biopsy needle, such as the design we are proposing, is passed through the interior channel of the endoscope. The channel allows for the safe passage of the needle, which exits the head of the endoscope by approximately 3cm. Once the needle is inserted into the endoscope, the cutting section of a biopsy needle pierces tissue and retains a sample (Figure 5). While a doctor views the subsurface image using ultrasound, this procedure is repeated until an adequate amount of tissue has been obtained or until the limits of acceptable patient trauma has been reached.

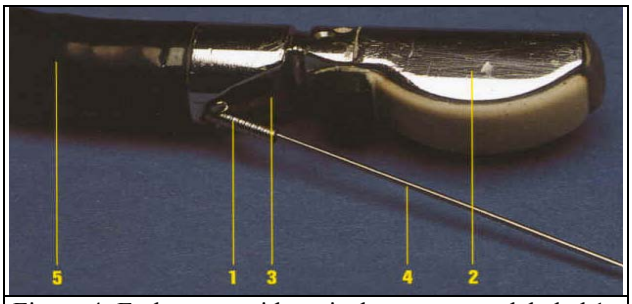

Figure 4: Endoscope with typical components labeled 1. Sheath, 2. Ultrasound transducer, 3. Optic lens, 4. Steel needle, 5. Distal flexible end of the endoscope. (Source: Endosonograpy.dk[4])

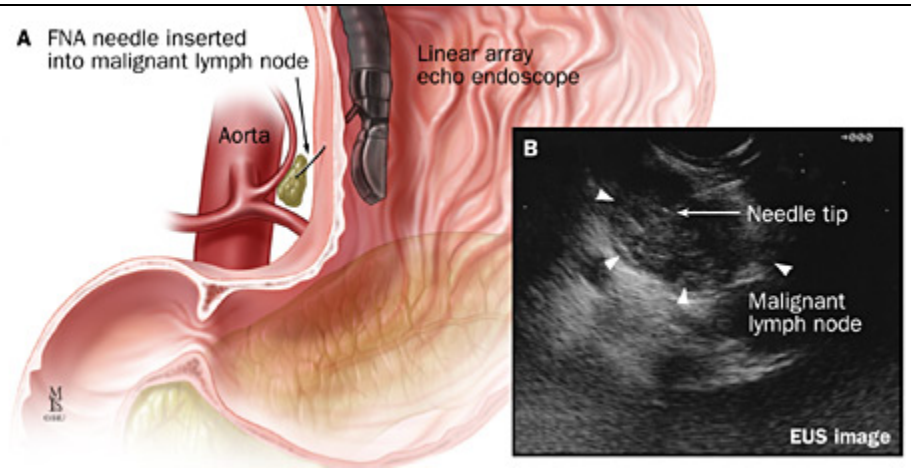

Figure 5 A, Technique of fine needle aspiration (FNA); B, corresponding endoscopic ultrasonography image. Source: Johns Hopkins Medical Institutions Digestive Disease Library

The endoscopy procedure and endoscope design enforce some constraints on the design of a needle biopsy device, such as overall size and shape. A needle must fit inside the endoscope and be long enough to reach a lesion. This needle must be able to cut tissue while maintaining its own structural integrity and ensure an acceptable level of medical safety. These are general assumptions that can be made for any sort of endoscopic tool.

2.3 Ultrasound Imaging

Once an endoscope is visually positioned in the general area of a suspected problem area, ultrasound imaging is used to gather information about the location of organs and tissue through the stomach and intestinal walls. This is accomplished using a small ultrasound transducer on the head of an endoscope that transmits a pulse of 2-5MHz for abdominal diagnosis.[5] The characteristic impedance of tissue echoes back to the transducer, allowing a technician to see a rough image of surrounding tissue. Ultrasound imaging offers advantages such as no ionizing radiation or contrast material, minimal patient cooperation, real time imaging and detailed images of the relatively inaccessible pelvic region. Disadvantages include a limited depth of penetration and low spatial resolution, although recent developments in 3D ultrasound imaging are promising.[6]

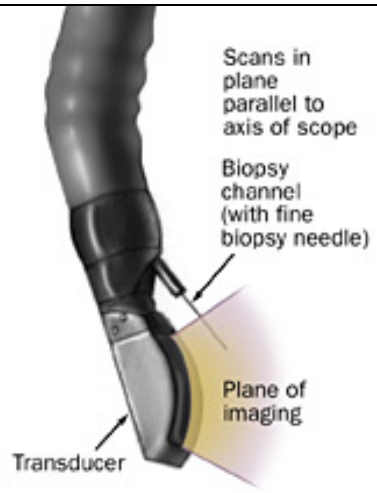

Figure 6: Endoscope with Ultrasound Transducer

Source: Johns Hopkins Medical Institutions Digestive Disease Library

From a design perspective, an endoscopic biopsy needle must be compatible with current ultrasound techniques by appearing in such imaging without distorting the view of surrounding tissue. *Echogenicity,* the ability of an object to be seen by ultrasound or the relative brightness of an object under ultrasound, is determined primarily by an object causing interference with ultrasound pulses. This occurs when objects have features of the same dimension as the incoming wave. A biopsy needle design may often have small features on the tip to increase its visibility under ultrasound compared to surrounding tissue. This may be done with a 150 grit blast to roughen the surface (Popper and Sons[37]), by coating the surface with a polymer that has small bubbles encapsulated within its coating, or with other features of the same scale. When designing new needle geometry, it would be useful to ensure that the design can use one of these processes or that the design itself may improve visibility.

Figure 7 Echogenicity of a dimpled needle.

Source: Relative Ultrasonographic Echogenicity of Standard, Dimpled, and Polymeric-coated Needles, JVIR, March 2000[7]

2.4 Anatomy and Biomechanics of the Gastrointestinal Tract and the Impact on Needle Design

In order to understand the functional requirements of an endoscopic biopsy needle, it is necessary to investigate the environment in which such a device will operate. The ability of a needle to successfully obtain tissue samples will depend on its interactions with human tissues. Differences in geometry and material characteristics of tissue

throughout the gastrointestinal system pose a significant challenge to the design. Moreover, tissue parameters inherently vary from individual to individual, and the diagnosis of abnormal tissues suggests that sample tissue characteristics may fall outside of the expected range even when normal patient variations are considered. Despite such a challenge, it is useful to understand something of the general anatomy and mechanical properties of the gastrointestinal tract that relate to the endoscopic procedure.

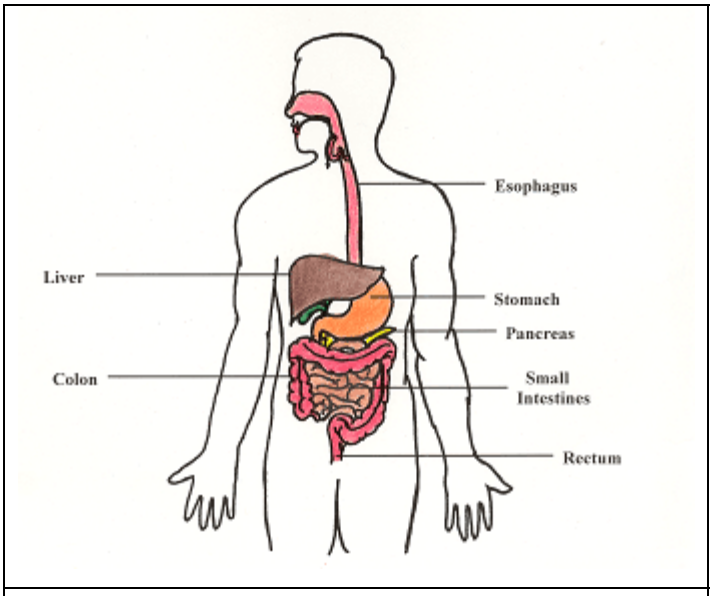

Figure 8: Major components of the gastrointestinal system

Looking at the basic function and size of tissues, the esophagus is a muscular tube, approximately 24cm long and 1.2 to 2.5cm in diameter, which transports food from the pharynx to the stomach [8], and limits both the minimum length and maximum diameter of an endoscopic tool. To prevent accidental tearing, which is common in endoscopic procedures [8,9], it is useful to know the average wall thickness of 4.8mm laterally and 3.8 mm posteriorly.[9] Following a small opening of the esophagus into the stomach, called the cardiac region, an endoscope would enter into the stomach itself. The stomach can range in volume 30mL for an infant, to 1500mL for an adult and maintains an extremely acidic pH of 1.5-2 in order to break down food so that nutrients can be absorbed through the intestines. The acidic environment limits the type of material that can be used for a

biopsy tool to corrosive-resistant materials, such as 300 series stainless steel. The volume of the stomach and the angle of entry require a small radius of curvature to access all areas of the stomach wall.

Once an endoscope is positioned within the stomach, a core biopsy needle would pierce through the stomach wall to obtain samples of nearby organs. The liver, which lies in the upper right of the abdominal cavity and important in breakdown of materials in the blood, is often sampled to evaluate its epithelial cells, which make up most of the organ structure. [10] The pancreas, which is the largest digestive gland (12 to 15 cm long in adults), is responsible for secreting enzymes that break down lipids, and proteins. According to Gray's Anatomy, "the spleen consists of a large encapsulated mass of vascular and lymphoid tissue situated in the upper left quadrant of the abdominal cavity between the fundus of the stomach and the diaphragm."[11] A core needle biopsy of the kidneys and other organs can also be performed using an endoscope depending on the organ's location within the body.

Because the endoscopic needle biopsy procedure often requires piercing through the stomach lining as well as the organ or interest, it is important to note the tissue cutting properties of organs. Mechanical properties of tissue can vary widely within the gastrointestinal system, and from patient to patient, making proper cutting force determination very difficult. Yamada's Strength of Biological Materials[12], which provides tensile properties such as ultimate tensile strength, ultimate percent elongation, and tensile breaking load for many tissues in the body. Where data is human data is scarce, estimates based on bovine and porcine experiments provide reasonable estimates of tissue properties for some internal organs[18]. Data from Okamura et al has noted puncture forces for bovine liver from 1N to 3N, and preliminary puncture tests for 19-Gauge needles estimated 0.1N to 1N (Appendix A) An abbreviated table of relevant data adapted from Yamada is shown in Table 1.

Table 1: Mechanical properties of the gastrointestinal system of an average adult. (Compiled from Yamada). [8]

Organ	Tensile Breaking Load (g/mm^2)		Ultimate Tensile Strength (g/mm^2)		Ultimate Percent Elongation	
	Longitudinal	Transverse	Longitudinal	Transverse	Longitudinal	Transverse
Esophagus	162	50	60	18	73	124
Stomach	131-147	112-119	46	38	89	107
Small Intestine	68	64	56	53	43	89

2.5 Pathological Examination

A biopsy is characterized by the removal and examination of tissue, cells, or fluids from the living body[13]. From these pieces of information, doctors can determine if the sample tissue is typical of that organ or potentially cancerous. To perform reliable chemical tests and to observe cells under a microscope, a minimum amount of tissue (approximately 15mm long and 1mm in diameter) is required.[14] While the details of how pathologists analyze tissue are complicated, the basic understanding of what they need from a sample is not. Doctors use biopsy samples to analyze the cellular composition of tissue and, in the case of a core needle biopsy, the structure of the tissue. Further information about the histology, the structural organization of cells, can be studied if a sample is preserved in the same volumetric configuration as originally within the body, which is possible with core biopsy needles but is often destroyed with aspiration of the sample. At the same time, other than extracting a group of cells, a biopsy should not alter the physical or biological characteristics of the sample, such as would happen in the presence of chemicals, abnormal temperatures, or if separated from the body for extended periods of time. A successful biopsy device would have to consider all of these requirements in addition to those that would allow it to travel through an endoscope.

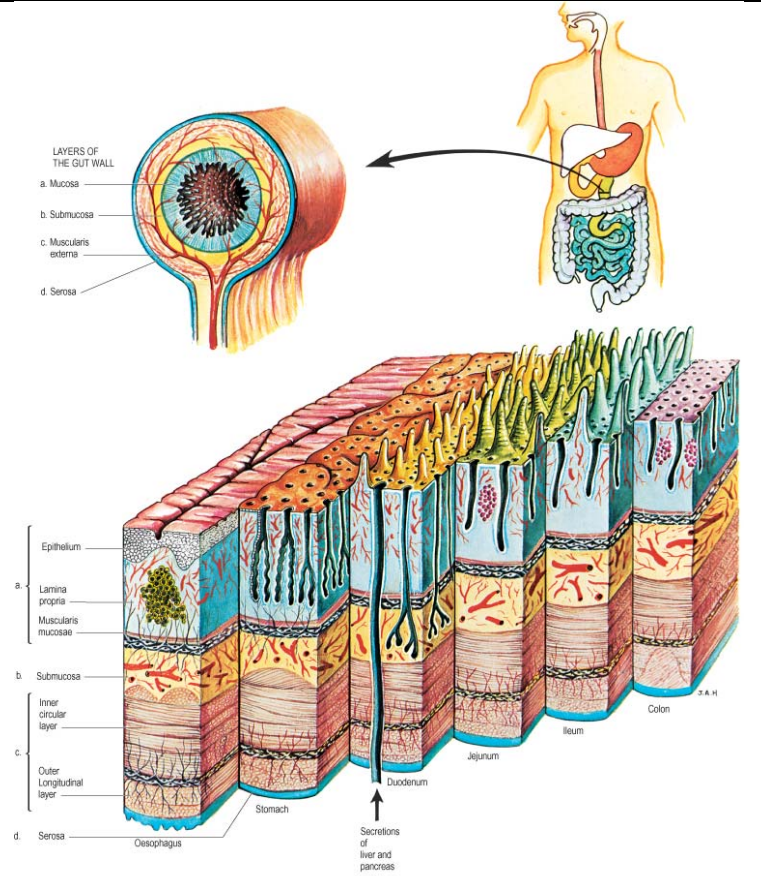

Figure 9: Layers of the Gut Wall . Source: Gray's Anatomy

2.6 Establishing Functional Requirements and Design Parameters

The endoscopy procedure and endoscope designs (Figure 4) place geometric constraints on the design of a needle biopsy device, such as the maximum needle diameter and minimum required sample length. The background information discussed in previous sections allowed the author to identify functional requirements; properties that a design would want to have in order to benefit the user. Design parameters, which quantify the functional requirements into engineering metrics, were also determined as shown in Table 2.

Table 2: Functional Requirements of Endoscopic Biopsy Needle	
Functional Requirements	**Design Parameters**
Fit within an endoscope to reach desired sampling site.	Minimum Endoscope channel diameter: 2.0mm (Hitachi[15]) Endoscopic biopsy needle outer diameter 1.06 mm 19-Gauge (Brugge[16]) Needle length: 138-140mm. (5cm past endoscope tube length) (Wilson-Cook [17]) Maximum bending radius approx. 5cm at tip. (Pentax Model)
Capable of Cutting Human Tissue (Stomach, Liver, Spleen, Kidney, Pancreas)	Cutting force greater than 5N. (Okamura[18]) Tip buckling force of >9N when extended. Provide a sample of approximately 15mm in length. (Bravo[19])
Accurate and Reliable	Cut only when at sampling site. Preserve tissue histology and diagnostic quality of sample Target sampling success rate of 80% (Brugge[16])
Interface/Feedback	Compatible with standard controls procedure for similar devices. Tip visible under ultrasound.

Requirements for an improved core-sampling biopsy needle were determined both through observations of current needle shortcomings, as well as through interviews with the potential customer[20], which here is specified as the gastroenterologist that would use an endoscopic biopsy needle for tissue examination. Because each biopsy procedure is costly and causes some patient stress, the overall aim of the needle was determined to be improved sampling reliability, measured as the average sample mass or length for a given needle gauge and wall thickness. These two measures, sample mass and sample length, would give the same sampling information because the combined gauge and wall thickness set the diameter of the sample. For a homogeneous sample of uniform density, the mass and sample length are proportional. Discussion with the customer set a target core sampling success rate of 80%. An overall 1.5cm desired sample length was set in order to provide an adequate amount of tissue for pathological testing. The needle diameter of 1.06mm (19 Gauge) would allow for standard endoscopic procedures. Of course, to ensure patient safety, the needle tip and any component of the needle cannot detach and become a threat to the patient during procedure. Finally, to allow for the doctor to maneuver the needle appropriately, the needle tip must be visible under ultrasound. With these basic requirements in mind, the following approach was taken to conceive, implement, and evaluate a core biopsy needle design.

Chapter 3

PRELIMINARY DESIGN ANALYSIS

In order to obtain a clearer understanding of our problem, initial tests were conducted with the biopsy needles presently used by doctors as well as other larger-scale methods of core sampling. This section describes the processes used to develop strategies, concepts, and, finally, an alpha prototype for proper tissue core extraction with desired histology.

3.1 Performance of Existing Needle Types

Initial design work focused on evaluation of current endoscopic biopsy designs and alternative strategies for improving tissue collection reliability. Current biopsy needles were classified into two main categories according to how they cut samples. End cutting needles punctured tissue using a sharpened hollow tube design to retrieve tissue. Side cutting needles use a sliding sheath to cut over an open side cavity in the needle. If either classification relied on suction to draw the sample out, the needle is termed an "aspiration needle."

A Wilson-Cook Echo 19 core biopsy needle (end-cut), a Wilson-Cook Quik-Core (end-cut), and a Boston Scientific percutaneous biopsy needle (side-cut) were used to gain an understanding of current technology and the limitations of existing designs. Not meant to compare individual manufacturers, this qualitative comparison allowed for the assessment of overall end-cutting and side-cutting ability. Sampling from store bought

calf liver, the Boston Scientific™ non-endoscopic side cutter was the only needle that produced a core sample that would indicate the tissue histology. The Echo 19™byWilson Cook™ produced poor samples and several attempts were needed before a sample was extracted. The Quick Core™ also by Wilson Cook™ produced no samples. Although post-mortem refrigerated liver may have different tissue properties, this introductory assessment allowed for some understanding of each needle's drawbacks.

Observations of the standard needles suggested that side-cut needles sometimes push tissue aside rather than cut through samples. Reasons can be lack of cutting speed, surface tension, and large radius of curvature of the tissue sample. End-cut needles that cored out a section of tissue were effective in cutting around the circumference of a sample, but they had no reliable feature that could then sever perpendicular to the cylindrical core. This resulted in a cylindrical cut at the tissue site, but sometimes no sample in the needle (Table 3).

Figure3: left) Boston Scientific™ Easy-Core side-cutting biopsy needle (www.bostonscientific.com), upper right) Close up of Side cut needle, lower right) close up of end-cut needle (www.wilconcook.com).

Table 3: General Description of Cutting Strategies	
Side-Cut	
Intended cutting	Estimate of Actual Cutting
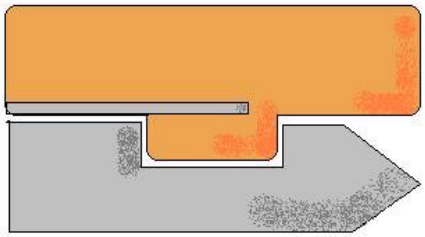	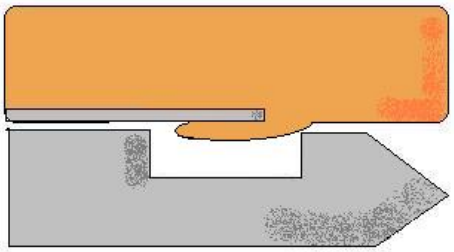
End-Cut	
Intended Cutting	Estimate of Actual Cutting
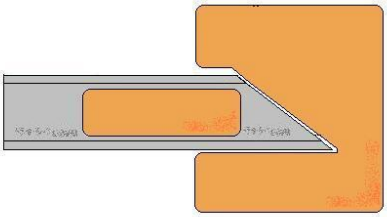	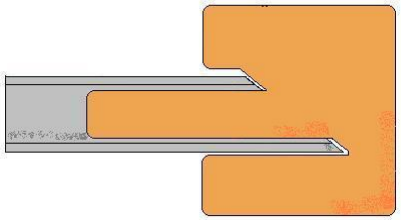

3.2 General Cutting Strategies

A focused brainstorming session was conducted in order to generate potential means of acquiring tissue samples, as seen in Figure 10, with additional ideas shown in Appendix B. Brainstorming also involved surveying aspects and methods of core sampling in fields outside of the medical industry. Topics that were explored include vibratory motion (to aid in endoscopic and tissue insertion), MEMS, ultrasonic cutting, suturing, and laser cutting. The resulting strategies were separated based on side-cut or end-cut classification, as previsouly mentioned. These two high-level groups were further subdivided according to the action associated with tissue capture: active (requiring some type of additional motion, moving component, or energy other than from the insertion/withdrawal motion) or passive (the action of inserting the needle into the tissue captures a sample without any additional effort, motion or action).

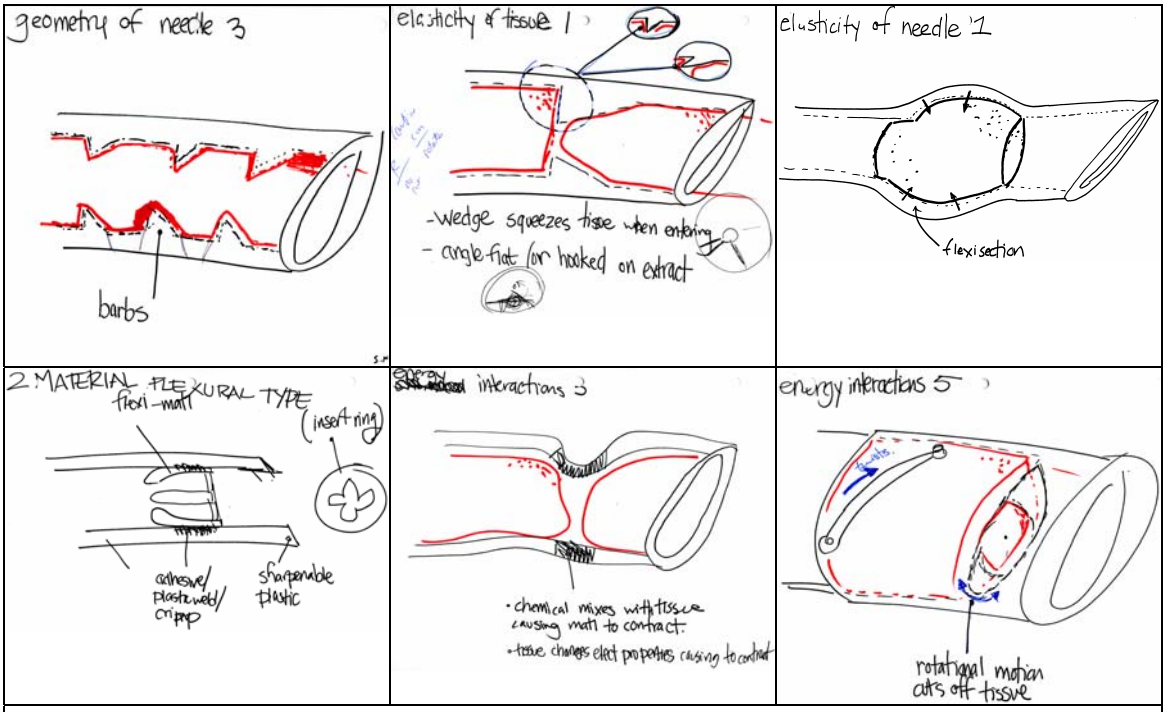

Figure 10: Sample of sketches from brainstorming session of tissue capture possibilities.

In order to select the optimal strategy to pursue, bench level experiments were performed. A qualitative method of comparing the extracted test samples was needed and so characteristics important characteristics were identified. These include the following:

- ease of motion for human interface (how well the doctor can control the device)
- manufacturability
- reliability (the consistency an accurate sample with desired histology is extracted)
- sample quality (how well the sample represents tissue histology)

In the bench level experiment, simple needle mockups, approximately 10x larger than the actual needle, were constructed from plastic tubes and tested on layered clay. The results were compared according to characteristics above and the end-cutting strategy was deemed easier to implement (Appendix C). The end-cutting strategy also tended to better preserve the layered clay histology when compared to the side-cutting strategy (see

Figure 6).

A passive means of extracting tissue samples was chosen based on size constraints and desire to limit complexity. Because an active method has moving parts or some energy source that could fail, they tend to be inherently less robust than passive methods. An active device would have to be consistently manufactured at less than 1mm in diameter to interact with the needle tip, and any bearing surfaces to support relative motion would have to be even smaller. A passive needle would have fewer components and no moving parts; could be safer for the patient and easier and less expensive to manufacture.

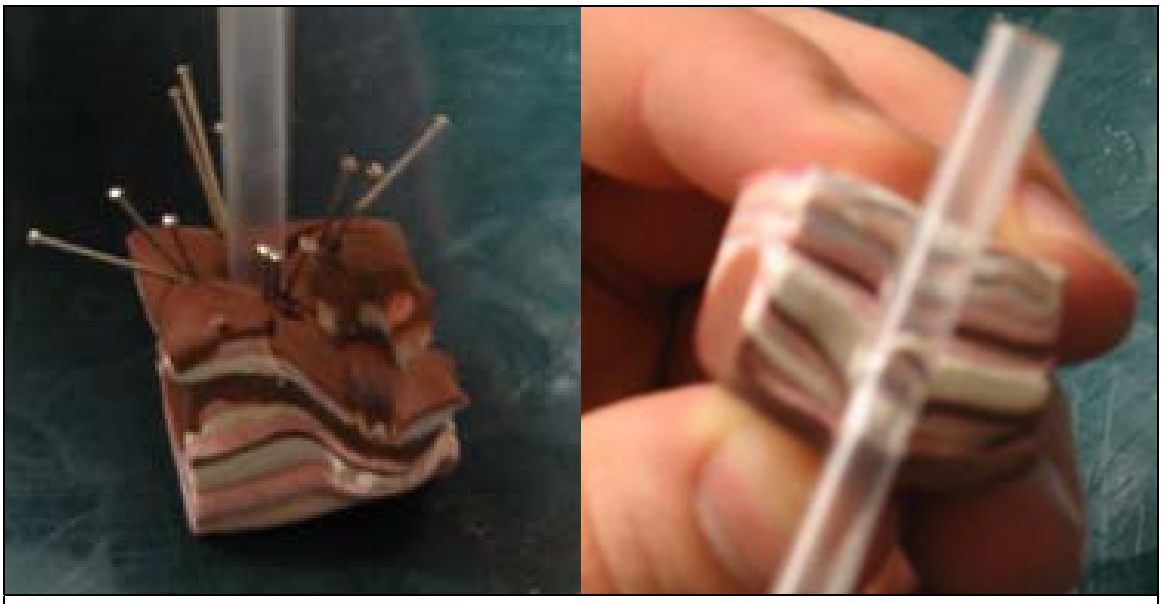

Figure 11: An experiment testing biopsy needle strategies: (a) an end-cutting strategy, (b) side-cutting strategy.

Following this design evaluation, first order estimates of the radial stresses and axial stresses during sample gathering were used to compare the strategies as seen in Figure 12. The difference between an active and a passive device was that the passive device used a radial force to sever tissue while the active devices would shear tissue. The end-cut strategy cut through the circular area ($\pi D^2/4$) of the tissue sample, whereas the side-cut

would have to sever through an area ℓ*D, where the length (ℓ) of the sample was $\ell \approx 10D$. In addition, passive methods would have to tear tissue in such a way that the tissue does not slip out of the needle before it is torn.

$\sigma_{passive\_endcut} \propto \frac{4\mu F_{radial}}{\pi D^2}$ (Eq. 1)	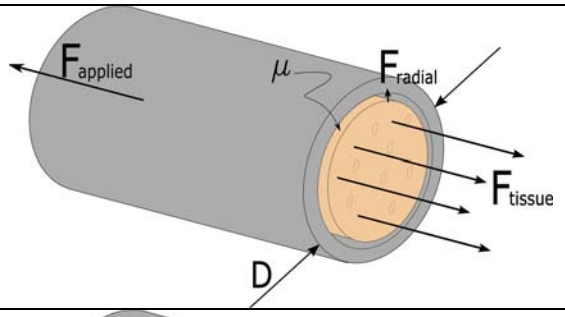
$\tau_{active\_endcut} \propto \frac{4F_{applied}}{\pi D^2}$ (Eq. 2)	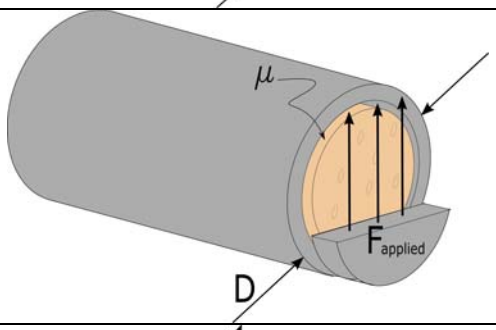
$\sigma_{passive\_sidecut} \propto \frac{F_{tissue}}{\ell D}$ (Eq. 3)	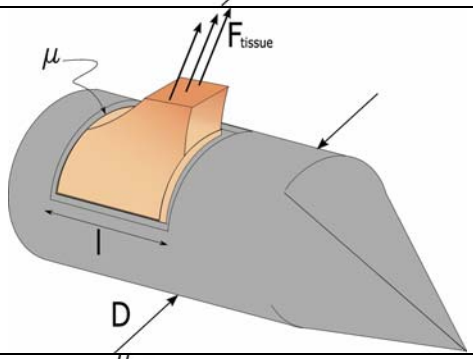
$\tau_{active\_sidecut} \propto \frac{F_{applied}}{\ell D}$ (Eq. 4)	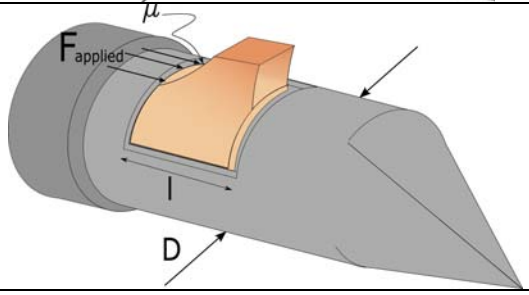

Figure 12: Cutting Strategies and First-Order Estimates of Cutting Force

The strategy with the minimum applied force that a feature would have to produce

from this estimate suggested the active end-cut had to shear the least to obtain a tissue sample. This was not surprising, since an end-cut would shear through a smaller cross section than a side-cut device that cuts along the length of the sample. This observation of an active device having a force advantage conflicted with bench-level experiments suggesting that passive devices would be easier to implement. A hybrid form of the end-cut design was introduced that would have no active components, but was capable of exerting force across the face of a tissue sample, such as was originally suggested by the active device equations. At the same time, it was realized that this force would only be advantageous when severing tissue, and could prevent a sample from entering the needle if present during the piercing stage of the biopsy action. Researchers hypothesized that a device that allowed tissue to enter the needle with little resistance but prevented tissue from exiting the needle by increasing resistance could act as a one-way valve to trap tissue. Concepts for an end-cutting needle built upon the idea of directional resistance feature.

A preliminary step in determining possible strategies involved analyzing the means in which a force is transmitted from the needle handle to the needle tip. The non-linear structure of the esophagus requires the endoscope and biopsy needle to trace a curved path and, therefore, the needle must then be flexible. With an assumed cylindrical shape, two motions were feasible: linear or rotational. In testing the feasibility of linear and rotational motion, the biopsy needle was bent in a similar manner as when inserted into a patient. The bend created a trivial increase in required force for linear motion. However, when attempting to revolve the bent needle, the 1+ meter length required substantial twisting (up to two revolutions) prior overcoming the frictional forces associated with the walls. This torsion-spring like behavior in the needle excluded revolving motions from possible cutting techniques. Although linear motion can be transformed into revolutionary motion, focus was directed towards pure linear motion to minimize complexity.

3.3 Evaluation of Needle Concepts

Following the end-cut strategy with differing entrance and exit resistances and a linear applied force, three directional biopsy tip concepts were developed and tested. Several types of passive end-cutting needles were machined using small metal tubing. The needles tested several sizes and cross-section shapes, but the critical variation was in the cutting mechanism. The cutting mechanisms can be classified as either internal barbs or crimped interference. Internal barbs created direct needle-tissue interference and relied on increase of friction to hold the tissue during extraction. The crimped interface used a smaller cross sectional area of the needle than the opening, resulting in tissue compression and increased wall friction during extraction. The crimped interface resulted poor tissue histology and this could be attributed to damage upon compression. As modeled, the barbed interface produced higher quality samples, as shown Figure 13; however, further testing was clearly needed.

Using the data from the machined metal needle experiment, the team decided on three concepts that had the greatest potential to retain samples reliably. In order to test these needle concepts, 4x scale parts were made using Selective Laser Sintering (SLS) and tested on a gelatinous phantom. The three concepts were as follows:

Figure 13: Experiment testing end-cutting biopsy needle concepts.

-A barbed needle with small internal features along the needle tip length that pointed radially inward. These barbs were also angled acutely into the needle such that a sample would be torn from the tissue when pulled out of the patient (Figure 14a). Inner features could be made by a punch method, with the outside needle wall covered by a plastic sheath to prevent tissue from escaping.

-A leaflet design consisting of a single ring of angled flexures that were intended to bend towards the needle wall so that tissue could enter when inserted into the patient. When pulled out of a lesion, these same flexures would bend towards the center of the needle to sever a sample within the needle. (Figure 14b)

-A tweezers concept, where a set of prongs compressed within the sheath of the needle. Once at the site of suspect tissue, the tweezers could be forced out of the sheath where the flexural prongs would expand to their unconfined shape. The sharpened end and inner lip on each prong severed tissue and the device captured a sample as the tweezers were pulled back into the sheath. (Figure 14c)

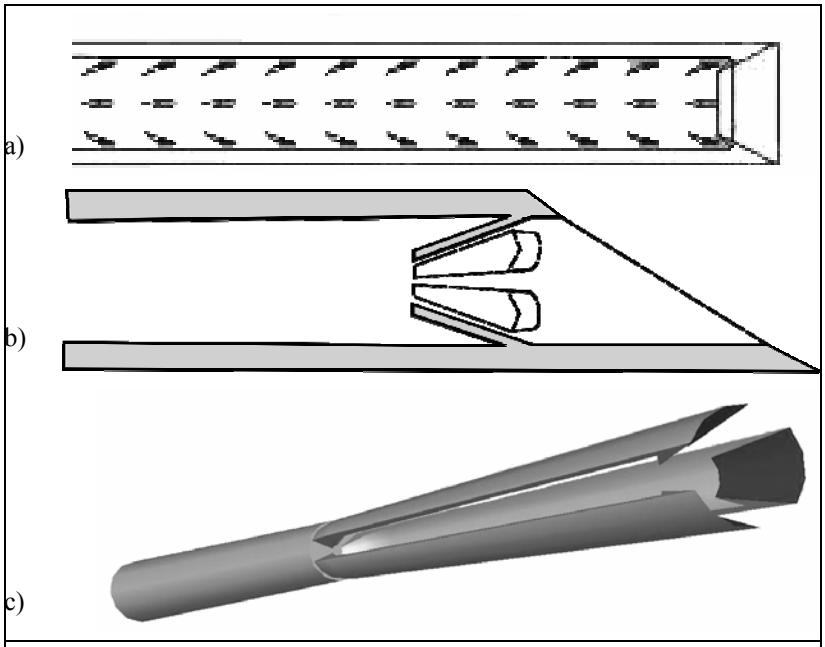

Figure 14: Needle Concepts a) Barbed Needle Concept, b) Flexural Needle Concept, c) Tweezers Needle Concept

The barbed needle prototype, containing four rows of 20 barbs, each with a 0.1mm diameter, was a simple design that required only a push pull motion. However, only a thin section of tissue was obtained. Also, although the concept successfully pulled out a core sample, this design did not ensure successful sampling because the tissue was often damaged upon removal from the needle.

The finger trap needle containing 6 flexible leaflets, illustrated in Figure 15b, also required only a push-pull motion to implement. Unlike the barbed needle, the core

samples were highly defined and it produced a sample more reliably. The volume of material was also, more intact as a core.

Positive results of the three-pronged tweezers concept, shown in Figure 15c, were that it cut the core of the tissue at the base and sealed the end of the needle using the principle of self-help. Unfortunately this design was difficult to operate, requiring three different motions that even the design team found to be confusing. Another disadvantage of the design was that the outward extension of the needle cut much more tissue than it captured, which was not desirable because it was more damaging to the patient. For these reasons, this design was considered to be less than optimal.

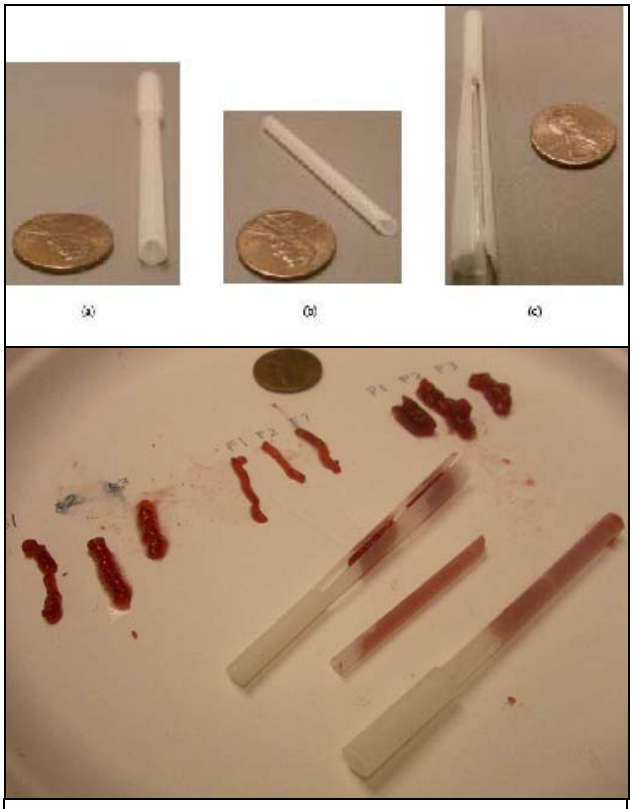

Figure 15: Prototype of three needle concepts and typical sampling results. a) Barbed needle, b) Flexural-member needle, c) Tweezers-type needle, d) Typical results using gelatin phantom.

Three samples from the results of the SLS experiment discussed above are shown in Figure 15d. Tests revealed that the flexural design produced the highest quality samples, followed by the barbed needle concept. These observations, in addition to concerns regarding the manufacturing of small directional inner features, lead to the final concept of the biopsy needle with internal flexures.

Chapter 4

FLEXURAL NEEDLE DESIGN PRINCIPLES

Following a concept that uses flexures to retain a core of tissue, some basic assumptions about flexure shape and deformation must be assumed. If a load is applied by tissue to the flexure, it is assumed that this force is distributed evenly among flexures. The flexure itself can be modeled as a cantilevered beam of uniform rectangular cross section with a distributed load normal to the flexure. Although larger deflections would be expected for the flexure than standard cantilever equations, these estimates give a basis for finite element analysis (FEA) of more complicated flexure shapes, larger deflections, and more complex loading scenarios.

4.1 Flexure Deformation

To design the flexural features, critical design parameters were identified to be flexure thickness (h), number of flexures (n) and the angle between the flexure and the needle wall (θ). In addition, the needle material's Young's Modulus (E) was considered an important factor, but this could be addressed for metal needles or even plastic needles, at a later time. The flexure thickness *h* would be approximately the same thickness as the needle wall for a metal design and possibly thicker for a plastic needle. The flexure width *b* was approximately the circumference of the needle divided by the number of flexures at its base and would have to narrow as it approaches the center of the needle to

prevent interference. The length of the flexure *l* was limited to the product of half the inner diameter of the needle and sin (θ). The tip deflection *d* of the flexure (assuming small deflections and a distributed load) was calculated from these values where the angle of the flexure changes depending on the direction of the applied force.

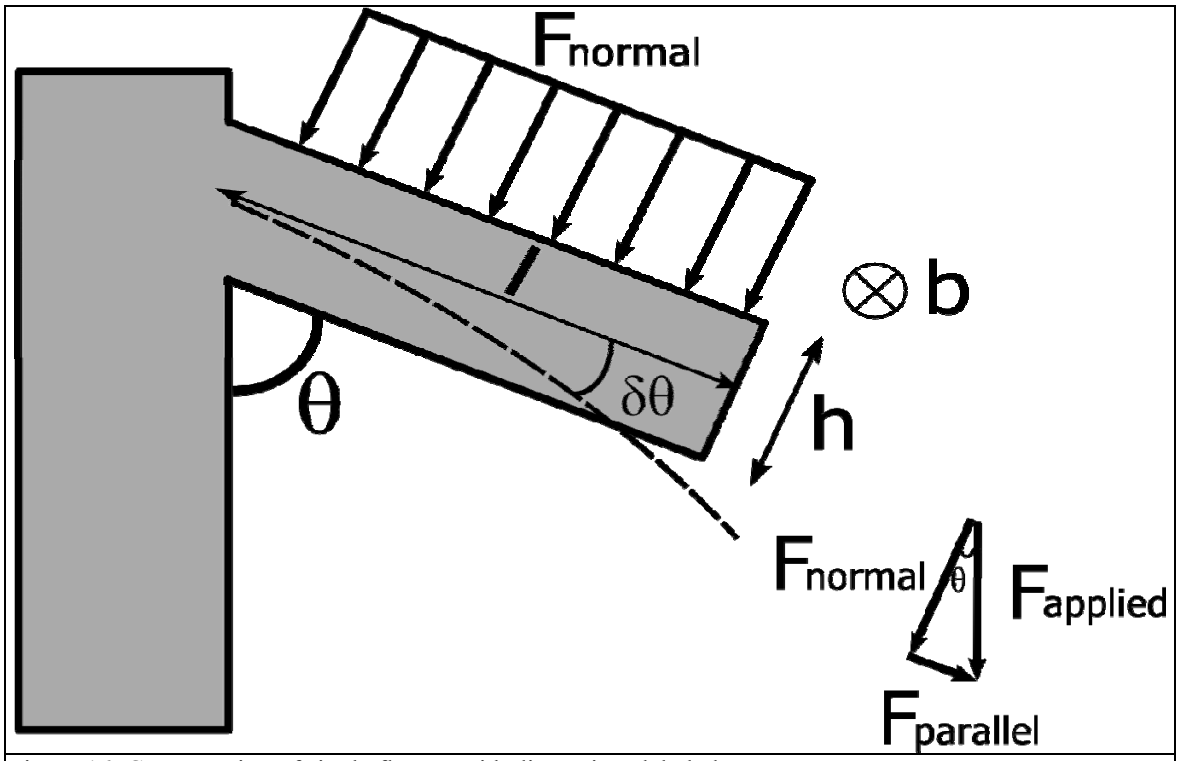

Figure 16: Cross-section of single flexure with dimensions labeled.

The normal force on a flexure when tissue enters the needle can be estimated from the normal force applied by the tissue divided by the number of flexures. This is multiplied by the sine of the flexure angle minus the difference in angle caused by tip deflection.

$$F_{entrance\_normal} \approx \frac{F_{applied}}{n} \sin(\theta - \delta\theta) \qquad \text{(Eq. 5)}$$

Similarly for the exit of tissue, the normal force is the applied force divided by the number of flexures and multiplied be the sine of the angle. The difference here is that

the angle of the flexure increases as a force is applied, which would cause the normal force to increase. The angle of the needle would also increase and tend to close off the inner diameter of the needle. Both of these factors would increase loading on the tissue, and encourage tearing.

$$F_{exit\_normal} \approx \frac{F_{applied}}{n} \sin(\theta + \delta\theta) \qquad \text{(Eq. 6)}$$

In order to estimate the deflection of a needle with dimensions identified in Figure 16, the moment of inertia of the needle, assuming a rectangular cross-section, would be:

$$I_x = \frac{bh^3}{12} \qquad \text{(Eq. 7)}$$

Finally, the tip deflection for a distributed load can be formulated using the equation below.

$$d = \frac{F_{normal}}{EI} * \frac{\ell^3}{8} \qquad \text{(Eq. 8)}^{21}$$

4.2 Parameter Variation

Using Design of Experiments (DOE) techniques[22], a 3x3 orthogonal array experiment was developed to determine a parameter configuration that would give the best biopsy performance by providing the longest intact tissue core sample, as seen in Figure 17. This data (Table 4) suggested that a needle with 4 flexures and a 45 degree angle to the inner wall was the most effective, with a 30 degree angle also more effective than a 60 degree angle. The best thickness for the flexures was inconclusive, which was considered

to be due to limitations of the SLA thickness.

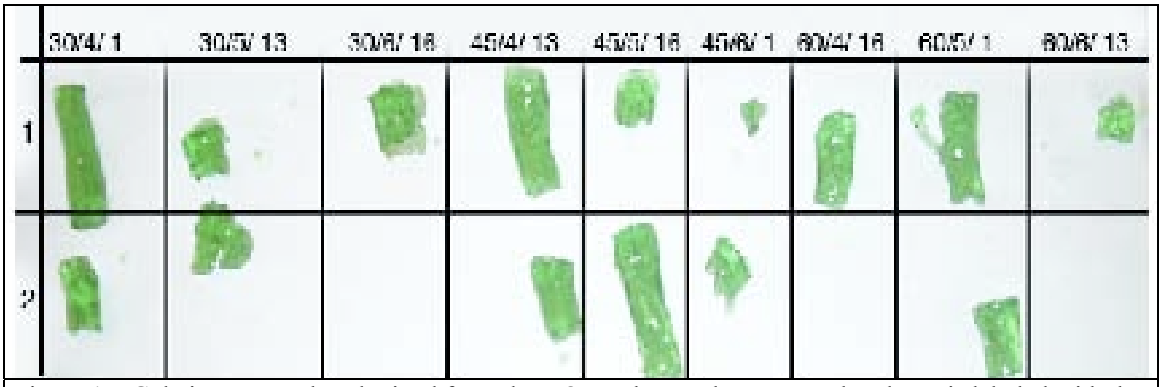

Figure 17: Gelatinous samples obtained from the DOE orthogonal array. Each column is labeled with the critical parameter values used for that experiment: (i) angle, (ii) number of flexures and (iii) flexure thickness.

Because the parameters of the flexure are interrelated, the balance between flexure stiffness and the needle dimensions are important to note. If one assumes that flexures are cut from the needle wall, increasing the stiffness by increasing the width (w) would lower the overall buckling strength of the needle by introducing a larger effective slit in the needle wall. In addition, increasing the needle stiffness by increasing the wall thickness (h), would also decrease the volume of tissue that can be acquired for a given needle gauge. Decreasing the length of the flexure increase critical buckling load, by creating a shorter slit in the needle wall, but comes at the price of a larger internal area through which tissue can still escape. Once the idea of a flexural member with in a biopsy needle was introduced, optimization of flexure parameters using FEA and additional tests was developed. This analysis is justified given the small sample size of initial tests (4 samples for each of 9 needles) and critical nature of the design.

Table 4: Design of Experiments 3x3 Orthogonal Array of Parameters Results.

Parameter	**Average**
3 variations	1=very good sample 4=little to no sample
Angle	
30	2.3
45	2
60	3
Number of Flexures	
4	1.6
5	2
6	3.6
Flexure Thickness	
0.1	2.3
0.13	2.6
0.16	2.3

Chapter 5

PROCEDURE AND TESTING OF 10X SCALE NEEDLES

In order to test the performance of the flexure geometry more rigorously, a set of stereolithographed parts were designed that allowed scaling of parameters. These prototypes were tested using a TA.XT Texture Analyzer[23] to obtain force deflection curves for the designs. The entrance and exit properties as well as sample weight were recorded.

5.1 Needle Variations

To test the tissue capture ability of the flexures as compared to a non-flexible member design, a wedge design was introduced. This wedge had the same overall angle as a flexure, but lacked the ability to deform when in contact with tissue. This could present itself as a simpler design that would lend itself to the benefits of injection molding. This extended wedge design was also introduced with angular variations and an extended section immediately following the wedge shape, which was meant to test whether the full wedge angle was significant in collecting tissue. Cross-sectional views of the needle variations tested are shown in Figure 18. A 10x coring needle with no inner features (not shown) was used to obtain a small number of samples during the force-deflection tests.

Needle Type	Angle	Model of Prototype
Wedge	30	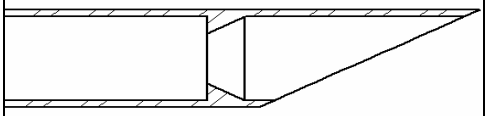
	45	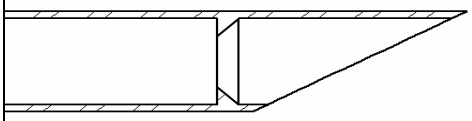
	60	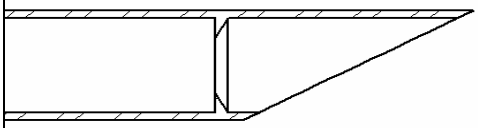
Extended Wedge	30	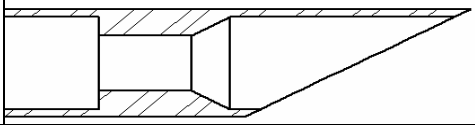
	45	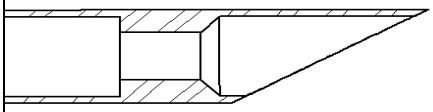
	60	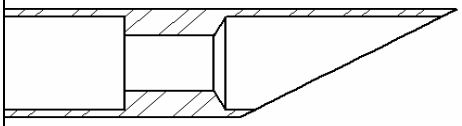
Flexure	30	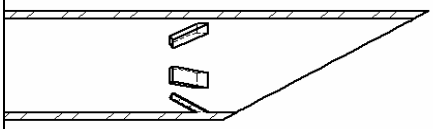
	15	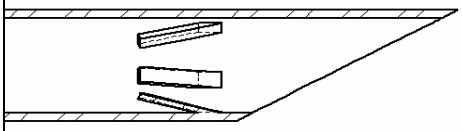
	30 Long	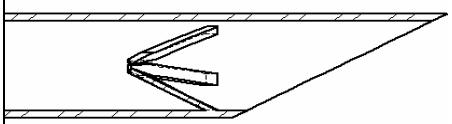
	15 Long	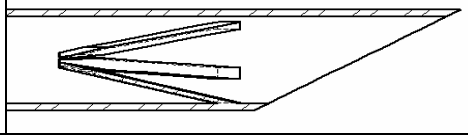

Figure 18: Needle Prototype Cross-Sections

5.2 Scaling of Needle Tip Prototypes

To verify dimensional parameters of the flexural needle design, a second set of prototype needles were also produced using a stereolithography process. Due to the resolution of this manufacturing process, which was limited to about 0.01" (0.25mm) in the z-direction (build direction) and 0.003" (0.09mm) in plane of the process[24] the needles were scaled so their critical inner feature was approximately 10 times the best SLA resolution. Dimensions were determined by matching the bending modulus (EI) for the scale needle using an approximation of $E_{sla} = 4.5x10^9$Pa for the stereolithographed parts and $E_{stainless_steel} = 200x10^9$Pa. Here *L* is the length of the needle cantilevered out of the endoscope.

$$F_{buckling} > F_{applied} \quad \text{(Eq. 9)}$$

$$F_{buckling} = \frac{\pi^2}{4}\frac{EI_{needle\_wall}}{L^2} \quad \text{(Eq. 10)}$$

$$I_{needle\_wall} = \frac{\pi}{4}\left(R_0{}^4 - R_i{}^4\right) \quad \text{(Eq. 11)}^{25}$$

By using the minimum resolution of the needle to set the inner radius R_i, and assuming an applied force of 5N, one can then match the I and E for the prototype to that of a stainless steel needle. This buckling equation assumes that the flexures are not cut from the needle wall, which would lower the overall buckling force, but this can be addressed by adjusting the cantilever length and inner diameter of the needle on the 1x scale.

5.3 Tissue Phantom for 10x Scale Needles

In order to approximate realistic tissue deflection and compression properties for the

unsharpened SLA needle designs on a 10x scale, a test material was needed that would deform more readily than actual tissue. A gelatin phantom was chosen for its relatively stable consistency at room temperature, and its shear and compressive properties that behave similarly to actual tissue[26]. The Young's modulus for gelatin has been shown to vary depending on pH, concentration, and loading frequency, with an estimate of 3.6kPa for 10% gelatin phantoms.[27]

Yamada et al. estimate the Young's Modulus of liver tissue around 30kPa, with other references giving 59kPa.[28] [29] References for the Poisson's ratio of porcine liver suggest 0.47±0.15 for elongation and 0.43±0.15 for compression.[30] A yield stress of 2.5×10^5Pa was also found in the literature.[30] These material properties may vary depending on frequency of the applied force, cutting speed, and because of inherent inhomogeneous properties of liver due to location and donor specimen condition.

Hertz contact estimates of the maximum shear stress τ_{max} allow one to compare the force (P) required to yield the samples by using an effective Young's modulus E^* to estimate deflection of both the needle and the tissue material. With the relative curvature of the contact surfaces (1/R) approximated using R equal to half the wall thickness, the following equation was used.

$$\tau_{\max} = 0.3\left(\frac{PE^*}{\pi R}\right)^{\frac{1}{2}} \qquad \text{(Eq. 12)}^{31}$$

For the case of a 1x stainless steel needle and a 10x SLA prototype:

$$\tau_{\max\_stainless\_steel} = 1600Pa \qquad \text{(Eq. 13)}$$

$$\tau_{\max\_SLA\_prototype} = 900Pa \qquad \text{(Eq. 14)}$$

5.4 Force Displacement Testing Setup

The eleven needle variations were randomly labeled and were tested using a TA.XTPlus with a 5kg load cell that was capable of measuring forces to within 0.1g. Each needle variation was plunged into a gelatin mixture that was prepared according to Knox Gelatine instructions[32], replacing juice with water, and allowed to cool for a minimum of 18 hours at 23.5°C as suggested.[33] Each prototype variation was cycled 40mm into the gelatin at a rate of 4.5 mm/sec and then extracted fully out of the phantom tissue. This was repeated ten times, each time at a new site approximately three needle-diameters center to center from the previous site, while measuring force and displacement of both the plunging and extracting movements. A standard coring needle with no inner features was used to obtain three samples for comparison of force and slope data.

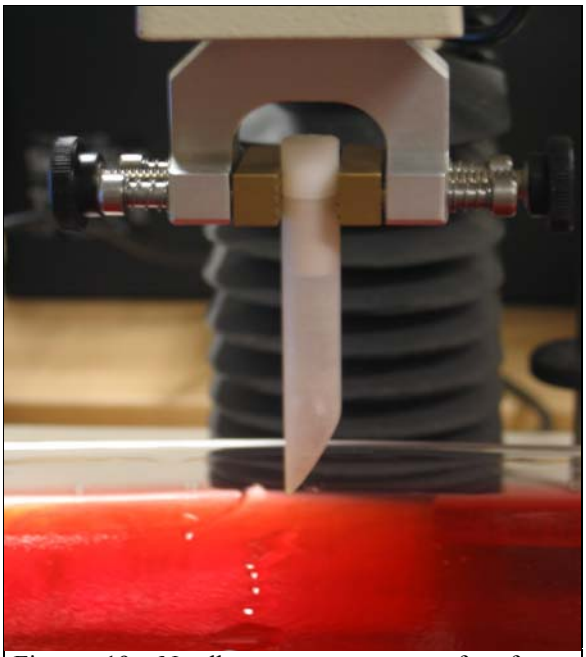

Figure 19: Needle prototype setup for force-displacement measurements

In order to subtract the friction that occurred on the outer wall of each needle, which would not be influenced by the internal features of either design, each needle was inserted into a previously punctured gelatin cavity while measuring force and displacement. Finally, the initial mass and final mass of the needles were measured to record the mass of gelatin that was captured for each sample. The needle designs were then evaluated based on their average mass of sample captured as a function of type (flexure, wedge, or extended wedge) as well as feature angle, which were 15, 30, 45 or 60 degrees relative to the needle wall.

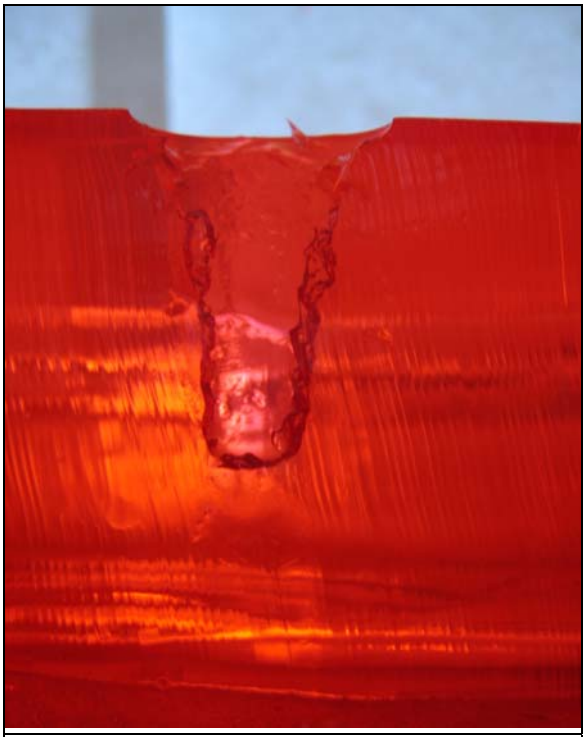

Figure 20: Cross section of gelatin phantom after coring test of 4x scale needles.

5.5 Force Displacement Data Results

Force displacement curves were compared according to overall shape by characterizing the piercing slope S1 (g/mm), the extraction slope in the region of tissue tearing S2 (g/mm), puncture force P1 (g), and frictional peak P2 (g) as shown in Figure 22. Similarly, the piercing slope S1' (g/mm) and extraction slope S2' (g/mm), as shown in Figure 21, was recorded for a pre-pierced gelatin site, which would indicate frictional characteristics of the outer wall. While Okamura et al.[18] list a quadratic relationship in the puncture step, a linear best-fit curve was used for the slope in regions where possible.

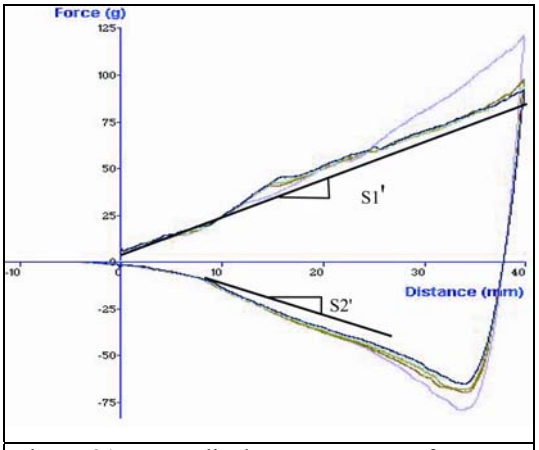

Figure 21: Force displacement curve of pre-pierced site showing slope from friction of outer wall, which is estimated using a linear best-fit approximation.

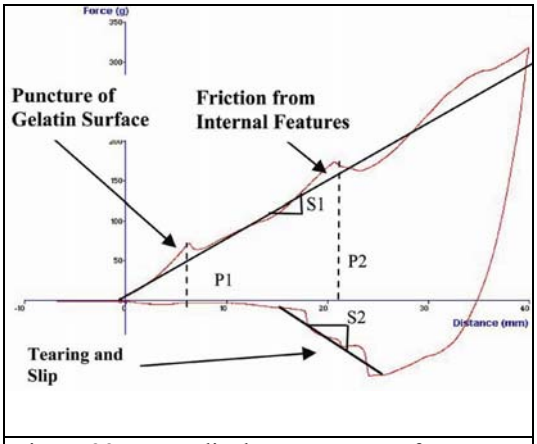

Figure 22: Force displacement curve for a flexural design with characteristic drop during needle puncture and sharp decrease in force during tissue tearing. Peaks from piercing and design features are also present.

Given the definition of the slope and peaks that were measured, data clouds for each needle type were plotted to compare the relative shape of the needle insertion and removal force-displacement curves (Figure 23-Figure 25). One would expect the initial piercing forces to be similar given that the only differences in the needle tip insertion would be due to prototyping error. However, once the gelatin entered the needle and came in contact with inner features, an increase in the measured force would be expected, and this is seen in curves below.

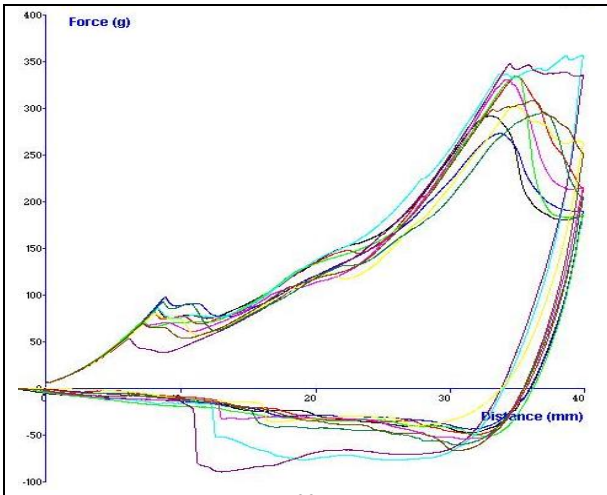

30

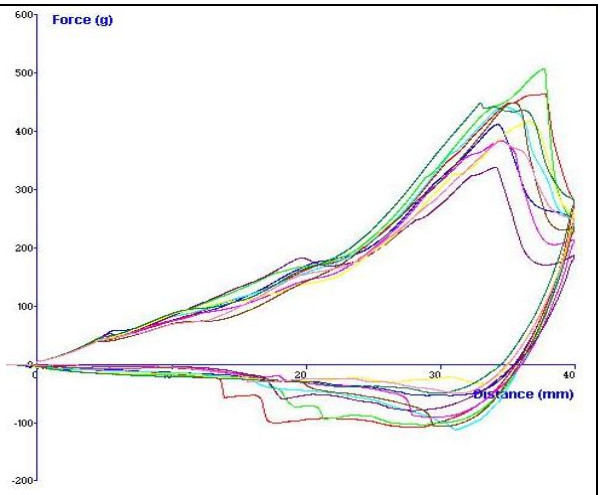

45

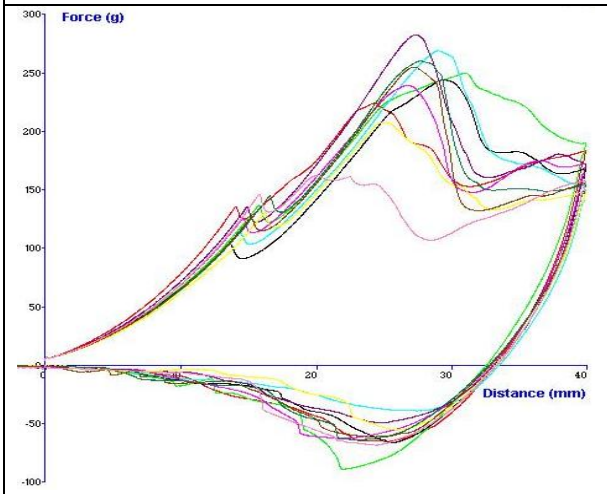

60

Figure 23: Force displacement curves for wedge needle prototypes for 30, 45, and 60 degree feature angles.

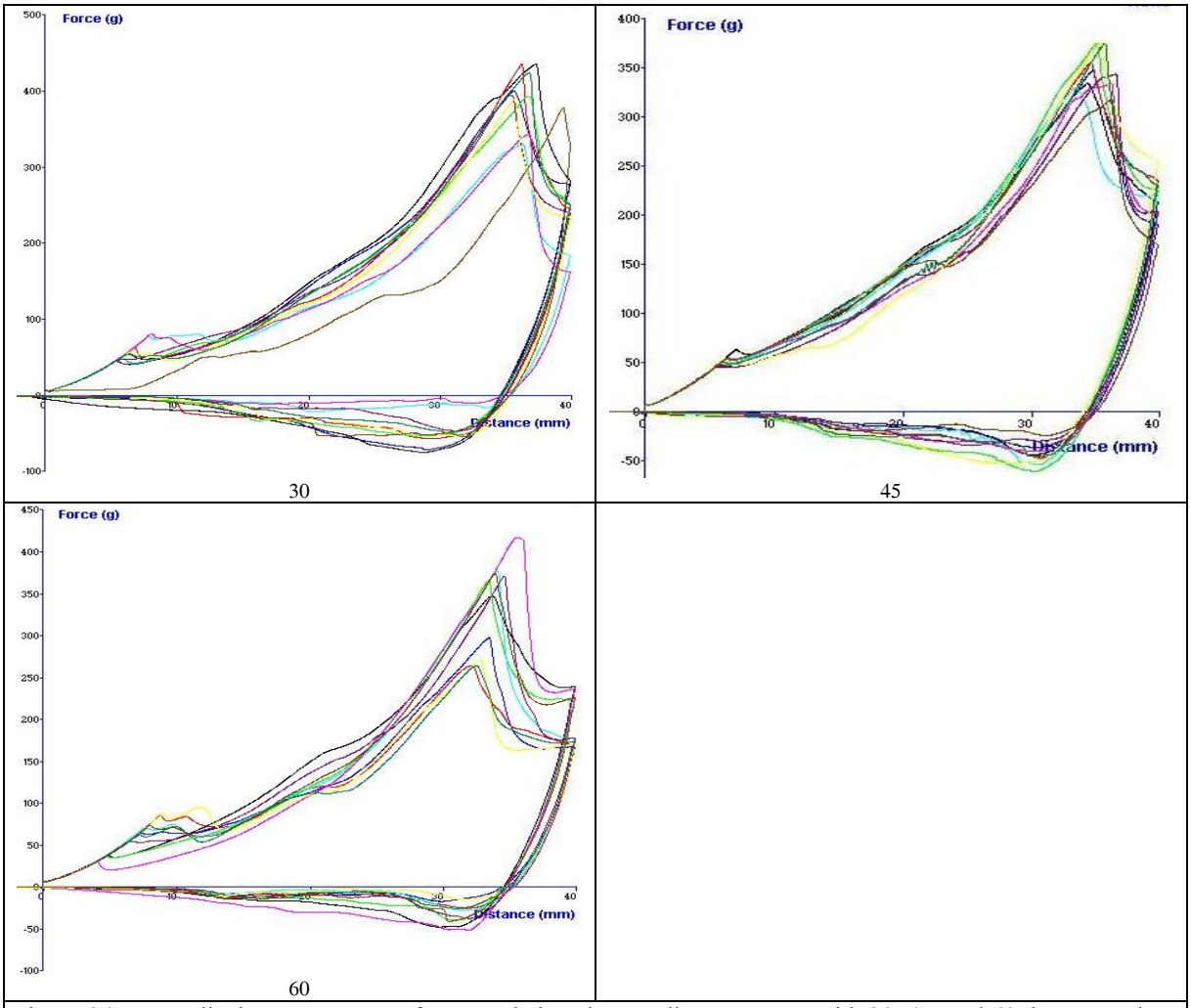

Figure 24: Force displacement curves for extended wedge needle prototypes with 30, 45, and 60 degree angles.

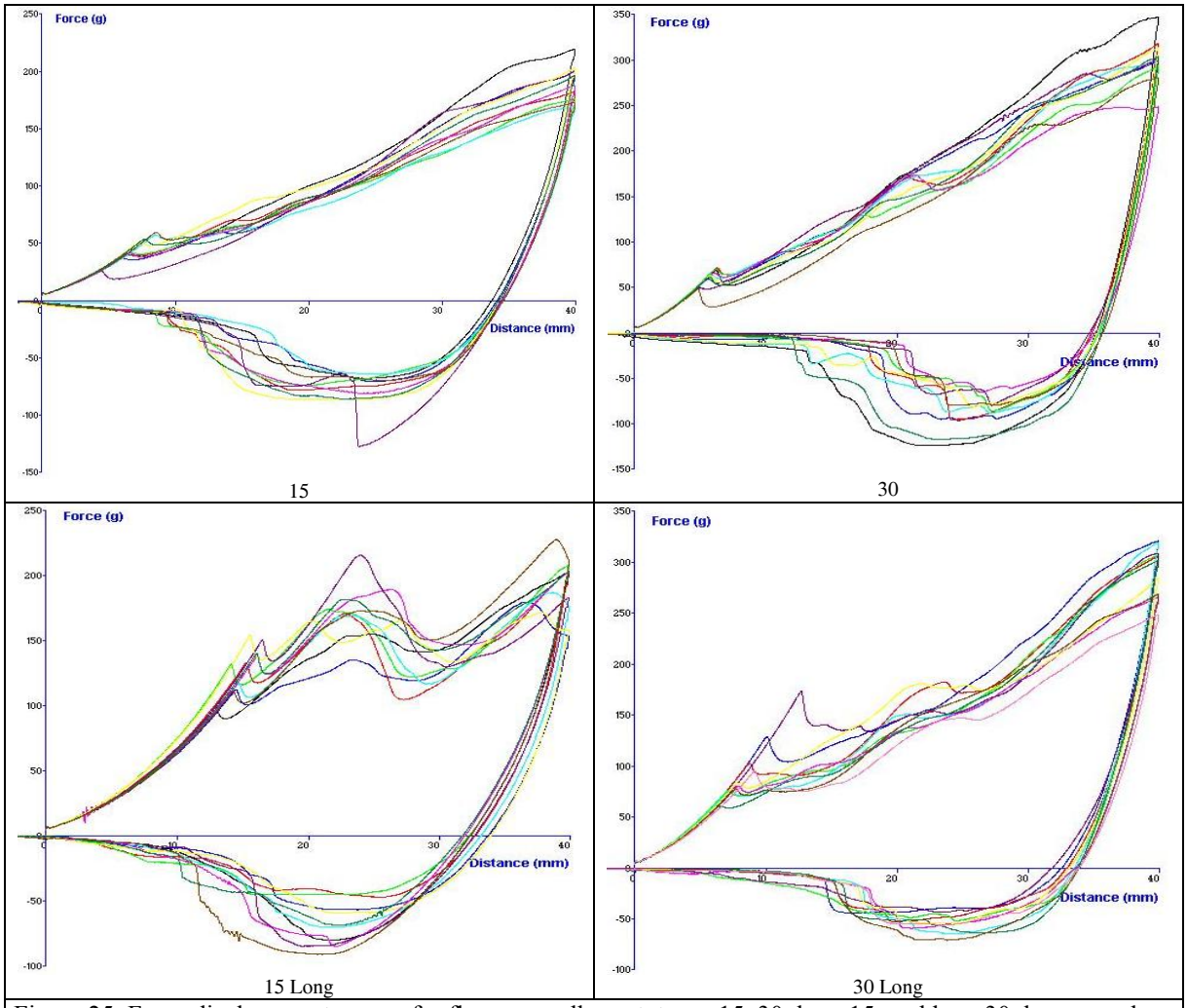

Figure 25: Force displacement curves for flexure needle prototypes 15, 30, long 15, and long 30 degree angles.

5.6 Sample Mass Comparisons for Design Type and Feature Angle

The average mass of sample gelatin collected by needles was compared to the feature type and feature angle to determine whether either parameter affected tissue collection. The number of the design for a particular design type was plotted in addition to the testing parameters and the number of each design that was prototyped so trends for each design were more evident.

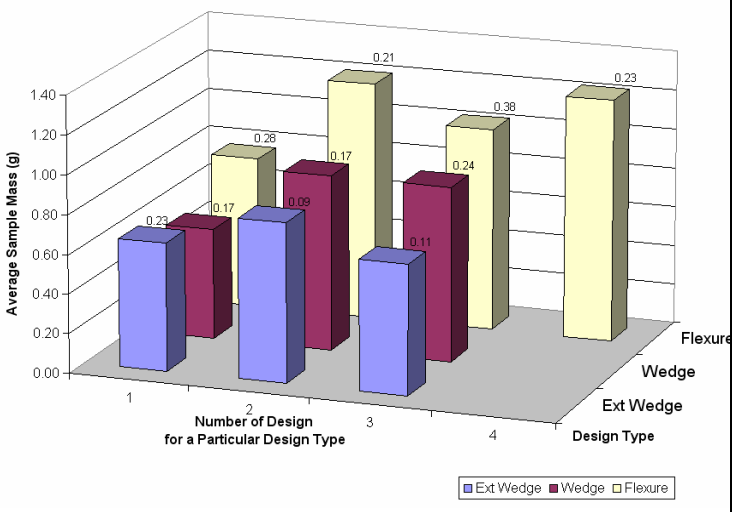

Figure 26: Average sample mass (g) vs. design type with a sample size of 10. Standard deviation noted above each data set.

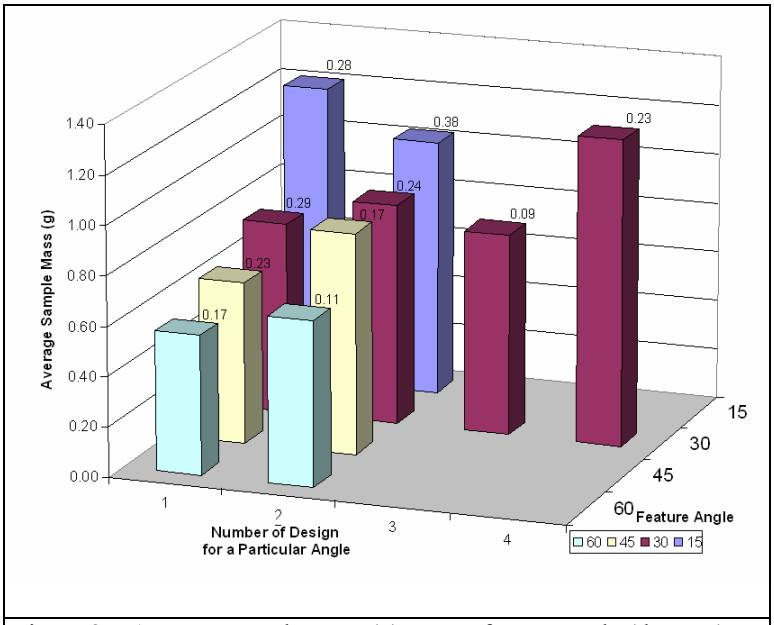

Figure 27: Average sample mass (g) versus feature angle (degrees) with a sample size of 10. Standard deviation noted above each data set.

The analysis of internal features for an endoscopic biopsy needle compared to average sample mass is shown in Figure 26 and Figure 27 according to feature type and angle. The average mass of a sample for a flexural needle design was 1.1g (σ= 0.21) compared to 0.78g (σ=0.19) for a wedge design and 0.71g (σ=0.09) for the extended wedge. It was also shown that the average sample mass was 1.1g (σ=0.08) for a 15 degree needle, 0.95g (σ=0.08) for the 30 degree needles, 0.77g (σ=0.04) for the 45 degree needles, and 0.61g (σ=0.05) for the 60 degree needles. The increase in sample mass with smaller angle and better results for a flexure suggests that the sample mass would be highest for a 15 degree flexural needle.

5.7 Puncture Forces for Design Type and Feature Angle

Force displacement results for the needle prototypes exhibited curves with a maximum piercing force of approximately 3N (300g), which scaled to the same order of

magnitude of the target max applied force of 5N, and fit within previously documented range for actual needle piercing experiments[18]. Therefore, the scaling appeared to be correct for the 10x needle and gelatin, which emulated actual size needles and tissue. The range of the peak piercing forces P1 from 0.44N-1.47N (45g-150g) estimated the 1N forces referenced by Okamura, and was close enough that it could be adjusted by altering the gelatin concentrations (Figure 28). The peak of the friction curve P2 had a dependence on the internal features. The lower peak for flexural designs as compared to wedge designs and the extended wedge indicated that the flexures did in fact exhibit a lower entrance resistance than either the wedge or extended wedge designs. The piercing peak P1, as would be expected, exhibited no dependence on the needle type.

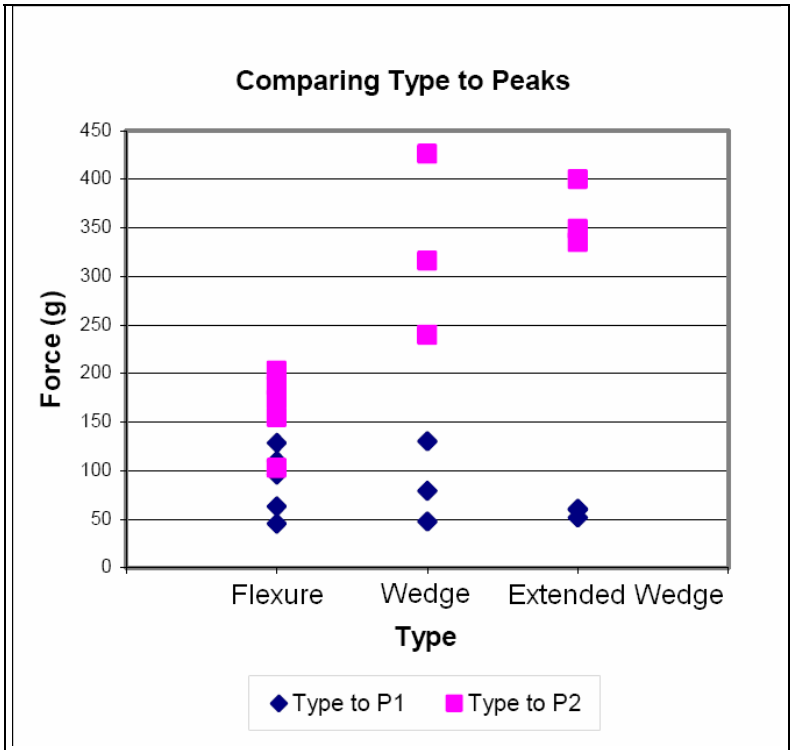

Figure 28: Comparison of Design Type to Characteristic Peaks

Also evident from the peak values of the curves in Figure 29 is the relationship between angle and peak friction force P2. As the angle increased, the frictional force increased for the needle sample. This matches the relationship described in Equation 5,

although the major improvement in peak friction was seen between 30 degrees with and average force of 1.9N (198g) σ=28 and 45 degrees with an average of 3.8N (388g) and σ=34, which is significant. As expected, there was no marked relationship between the internal feature angle and the puncture force P1.

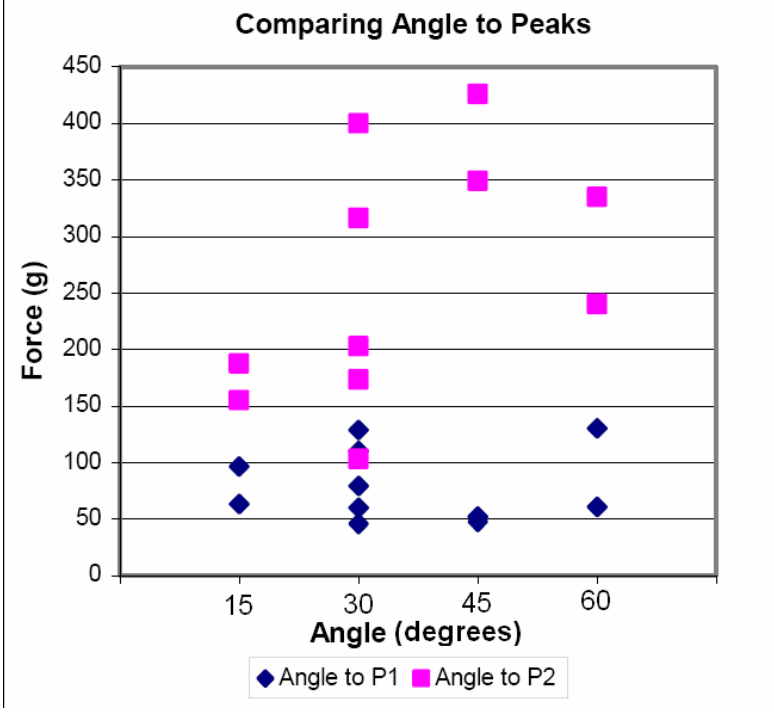

Figure 29: Comparison of Feature Angle to Characteristic Peaks

5.8 Entrance and Exit Slope for Design Type and Feature Angle

The slope of the force displacement curves during puncture S1 showed only a slight dependence on the needle type, as seen in Figure 30 and from the standard deviations in column 4 of Table 5 . This relationship was most likely a result of the characteristic peaks for each needle type weighing into the linear best-fit curve and not a direct result of the internal feature. This result is also supported by the idea that the linear curve is an estimation of wall friction, as described by Simone and Okamura34 and the puncture

force more closely fit a quadratic polynomial. Further, there was no effect on the slope of the pre-pierced site S1' as needle type varies, which was expected.

A relationship that was evident was the effect of needle type on the slope of the needle exit curves S2 in Figure 30. The flexure designs showed a larger magnitude slope of -4.0g/mm, followed by the wedge -2.8g/mm and the extended wedge -0.6g/mm designs. This abrupt change in force corresponded to a sudden failure in the gelatin, which was observed during testing, as opposed to a gradual sliding of the sample. This result suggests an increased likelihood of successfully severing a tissue sample, although the average standard deviation (σ=1.5) was rather high and would benefit from a larger sampling of needles.

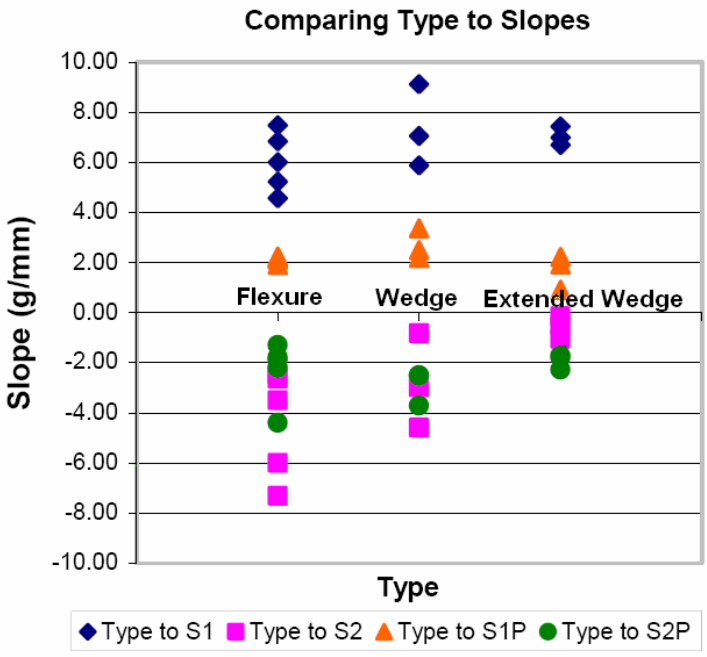

Figure 30: Relationship between Feature Type and Characteristic Slopes

The angle of the needle entrance created no noticeable difference in S1 and S1' (Figure 31). This corresponds with previous comments suggesting the linear slope is

related to wall friction, with piercing causing a quadratic peak.

There was a relationship between the exit slope S2 and angle, as was hypothesized. As the feature angle increased, exit slope decreased, which suggests that there was less tissue captured, and is also supported by the mass results reported previously. The inner feature angle had no effect on the slope of the exit curve in the pre-pierced case S1'.

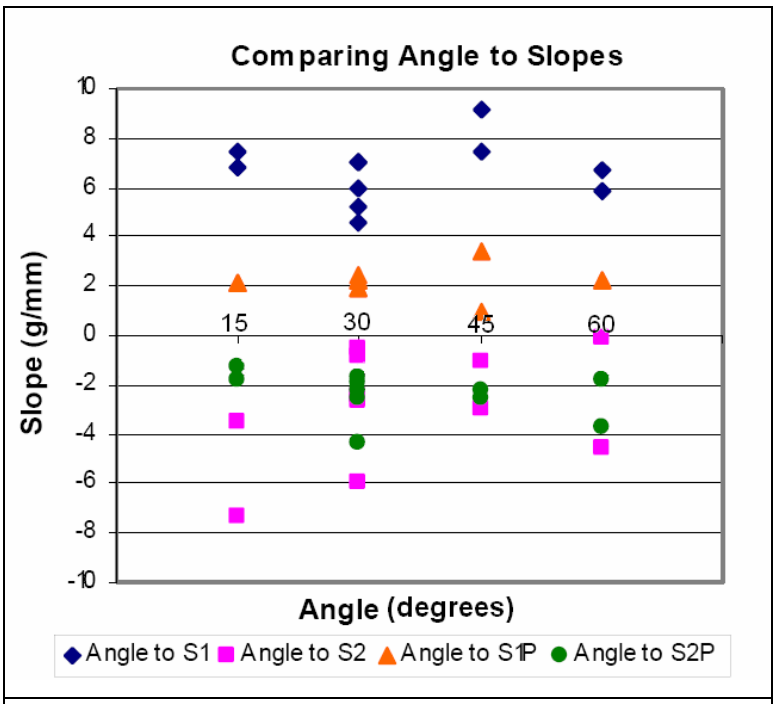

Figure 31: Comparison of Feature Angle to Characteristic Slope

These comparisons listed between feature angle and design type are summarized in Table 5, with the number reported for the piercing force and slope as the average of eight individual tests. The exit and entrance slopes S1' and S2', representing a previously pierced hole, are the average of five individual tests per needle. Data for the entrance and exit slope (S1 and S2) and puncture forces (P1 and P2) for the 30 degree extended wedge, as well as the pre-pierced slope (S1' and S2') for the 30 degree wedge, were obtained visually from a screen image of the graphs rather from tabulated data, so no standard deviation data could be provided.

Table 5: Entrance and exit characteristics of sample needles. (** indicates data not available)

Type	Angle	S1 (g/mm)	Std Dev	S2 (g/mm)	Std Dev	S1' (g/mm)	Std Dev	S2' (g/mm)	Std Dev	P1 (g)	Std Dev	P2 (g)	Std Dev
Standard Core	none	4.1	0.1	-1.75	0.7	**	**	**	**	56	10.5	59	4.41
Extended Wedge	30	7.0	**	-0.5	**	1.9	0.2	-1.7	0.3	60	**	400	**
Extended Wedge	45	7.4	0.3	-1.0	1.0	0.9	0.1	-2.3	0.4	52	5.1	349	20.8
Extended Wedge	60	6.7	0.8	-0.1	0.7	2.2	0.3	-1.8	0.1	61	20.4	335	55.7
Flexure	15 long	7.5	0.5	-7.3	2.0	2.1	0.4	-1.3	0.2	63	7.9	187	45.0
Flexure	15	6.8	0.5	-3.5	2.2	2.2	0.5	-1.8	0.5	96	33.2	155	16.3
Flexure	30 long	5.2	0.3	-2.5	1.5	2.2	0.2	-4.4	1.0	129	18.7	173	21.0
Flexure	30	4.6	0.3	-2.6	1.6	1.9	0.2	-2.2	0.2	46	10.3	103	40.2
Wedge	30	7.1	0.6	-0.8	1.2	2.5	**	-2.5	**	79	13.3	316	24.6
Wedge	45	9.1	0.9	-3.0	2.6	3.4	0.4	-2.5	0.2	48	6.1	426	48.1
Wedge	60	5.9	0.6	-4.6	1.3	2.2	0.3	-3.7	0.2	130	13.3	240	34.6

5.9 Visual and Audible Reference of Intended Operation

During testing of the 10x scale needles in gelatin, several unexpected indicators of a needle's sampling success became evident that could lead to other testing, which are mentioned below. The first was that, for a 10x scale needle, motion of the flexures was visible to the naked eye and could be photographed by a standard 3x zoom digital camera. This was aided by a coloring added to the gelatin test material. Secondly, for some of the more successful samples, an audible separation in the gelatin could be heard. Although statistical correlations for these indicators were not calculated, they served in some way as a measure for the operator of a "good" sample before a mass measurement was taken. An example of flexure deformation during testing is shown in Figure 32.

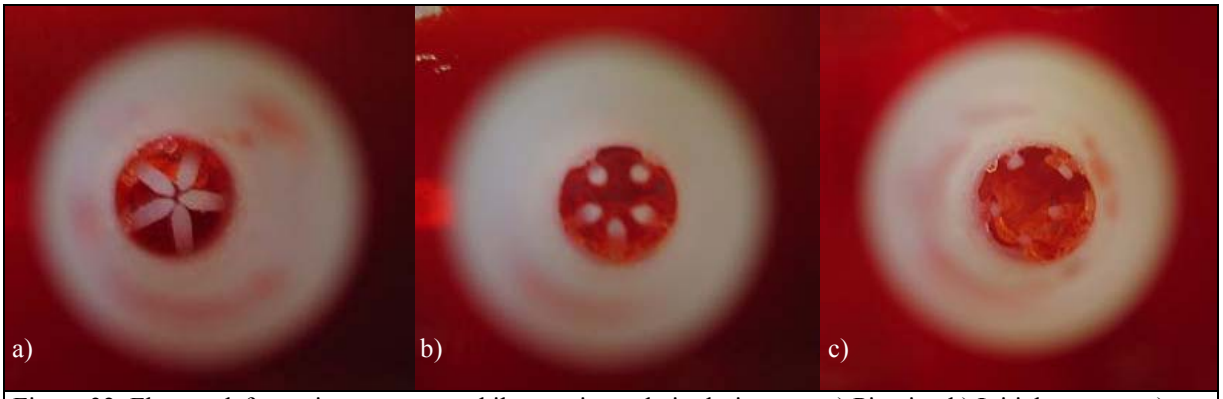

Figure 32: Flexure deformation sequence while entering gelatin during test. a) Piercing b) Initial entrance c) Sample collected prior to withdrawal & severing.

Chapter 6

FINITE ELEMENT ANALYSIS

This section discusses optimization of the needle tip flexure design through the use of finite element analysis. From Chapter 5, the results of the 10x scale prototypes indicated that the optimal configuration of the needle design would use flexures protruding from the inner needle wall at a 15 degree angle. The overall flexure width, initially estimated as a 30 degree section of the needle wall, and flexure length could still be adapted to provided better entrance and exit deformation. To further refine the flexure shape, CosmosWorks finite element analysis was used to find a design that was both able to deform and capable of withstanding the stresses created from an applied load.

6.1 Flexure Dimensions for Applied Loads

Because of the relatively simple shape of the biopsy needle flexures, estimating the flexure as a cantilevered beam with a distributed load as explained earlier in Section 4.1 , a simple Matlab script was initially used to estimate characteristics of the needle deformation by changing parameters such as applied force, number of flexures, flexure angle, flexure length and flexure width. Of course, there may exist several solutions for flexure shape that deform to the dimensions of the inner needle channel. What this section attempts is to approach a solution that compromises between a deflection of approximately 20% of the inner radius or 0.10 mm, while simultaneously withstanding and applied load of 1N without plastically yielding. Also, this flexure shape must have

dimensions that, when cut from a hollow stainless steel needle wall, do not cause the overall needle length to buckle.

To accomplish such a task, a simple Matlab script that allowed the user to alter input parameters was implemented (Appendix D). The script was compared to a CosmosWorks finite element model to compare maximum deflection, which would of course occur at the tip, and maximum stress, which one would expect on the upper portion of the flexure closest to the wall of the cantilevered section. Because there were many parameters that could be adjusted to accomplish the desired outcome, several assumptions were made. First, the number of flexures, four per needle, was chosen from success with previous design of experiments tests. However, the same analysis could have been done for one to six or more flexures, as long as the outer needle could still withstand buckling. The thickness of the flexure was set as the thickness of the needle wall, which stems from the assumption that the flexures will be cut from the needle wall. The current needle wall thickness, which was chosen to match a Cook 19-gauge endoscopic biopsy needle, for comparison, used an extra thin wall (19XXTW) T304 stainless steel with inner diameter of 0.9271 mm to 0.9779mm (0.0365in-0.0385in). Material properties listed from the manufacturer[35] for T304 Stainless were also used in the FEA model. (Appendix E)

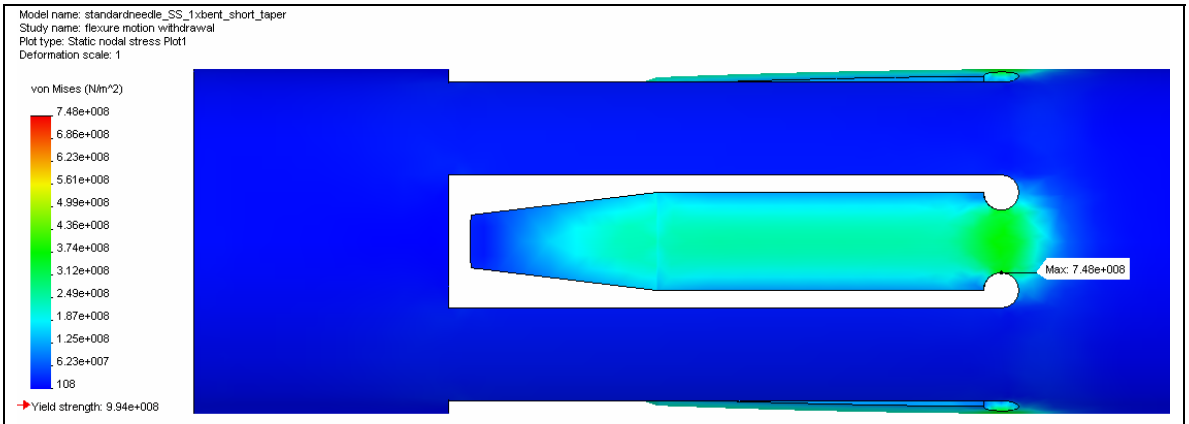

Figure 33: Stress analysis in CosmosWorks of tapered flexure with 2N applied load and 15 degree bend on tapered section.

After a series of 22 iterations, which included lengthening the flexure into the needle wall as will be explained in the next section, the final needle dimensions were determined. The final needle included four flexures with a width of 0.3026mm (30 wedge of circular cross-section). These flexures had 0.6mm of length bent at a 15 degree angle into the needle, with another 1.0mm of the flexure cut into the needle wall but not bent. This allowed a 2N applied force, which is the largest the flexures would be expected to see when cutting liver tissue, to deflect the needle tip by a 0.053mm relative to the needle channel, while causing a maximum stress of 7.48×10^8 N/mm^2. This is below the 9.94×10^8 N/mm^2 rating of the vendor, and includes some conservative estimates for safety due to the fact that the needle tip would see most of the entrance force when cutting.

6.2 Windowing Flexure Parameters to Prevent Buckling of Needle Wall

With dimensions estimated from the FEA model shown in Figure 33, a model of the needle tip buckling gave loading estimates for the remaining portion of the needle shaft. The needle length was assumed to be 38.1mm (1.5in) based on the length of a biopsy needle that would extend past the endoscope during a biopsy procedure. The buckling model assumed a fixed constraint on the back end of the needle and that the needle tip was fixed in the plane orthogonal to the needle axis.

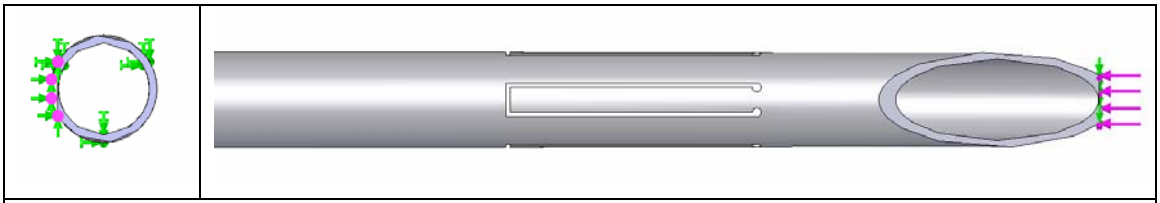

Figure 34: Forces and restraints on needle design with worst-case dimensions for needle buckling

A 5 Newton force was applied to the needle tip and a load factor was given that would estimate the buckling force according to Equation 15.

$$Fbuckling = Fapplied * LoadFactor \quad \text{(Eq. 15)}$$

With a 5N applied load, a Load Factor of 9.07 estimated from the FEA suggested that the design from Section 6.1 could withstand an applied load of 45 Newtons before buckling. Because 5 Newtons was estimated as the maximum expected load, the load factor is essentially the safety factor for buckling of the needle tip. It should be noted however, that loading conditions such as a bending moment applied to the needle, could reduce the maximum sustainable force significantly.

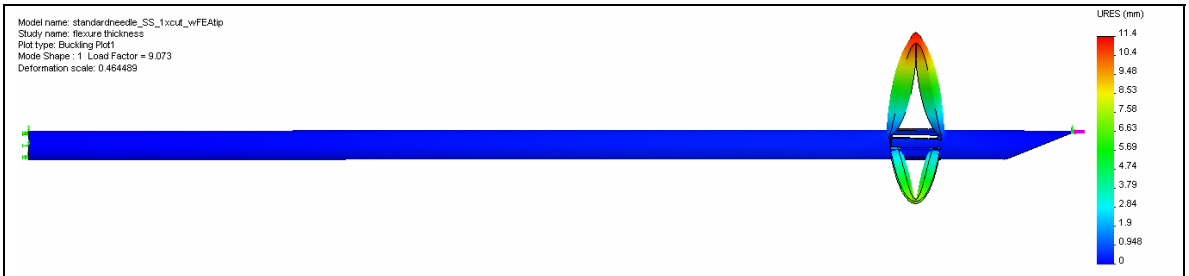

Figure 35: Buckling analysis estimate of failure for 1st buckling mode with deformation scale of 0.46 and load factor of 9.07

6.3 Optimization of Flexure Shape to Prevent Plastic Yielding

The desired goal in further optimizing the flexure design was to maximize the tissue extraction ability without causing detrimental needle deflection. After analyzing the stress distribution of the flexures, it was determined that varying the geometric shape of the flexure could reduce the associated stress and prevent plastic deformation.

a)

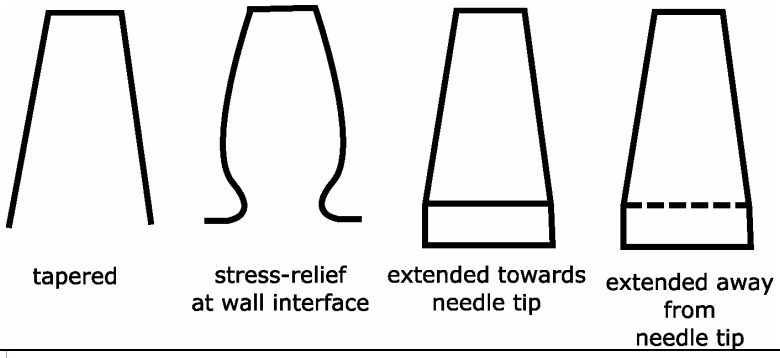

b)

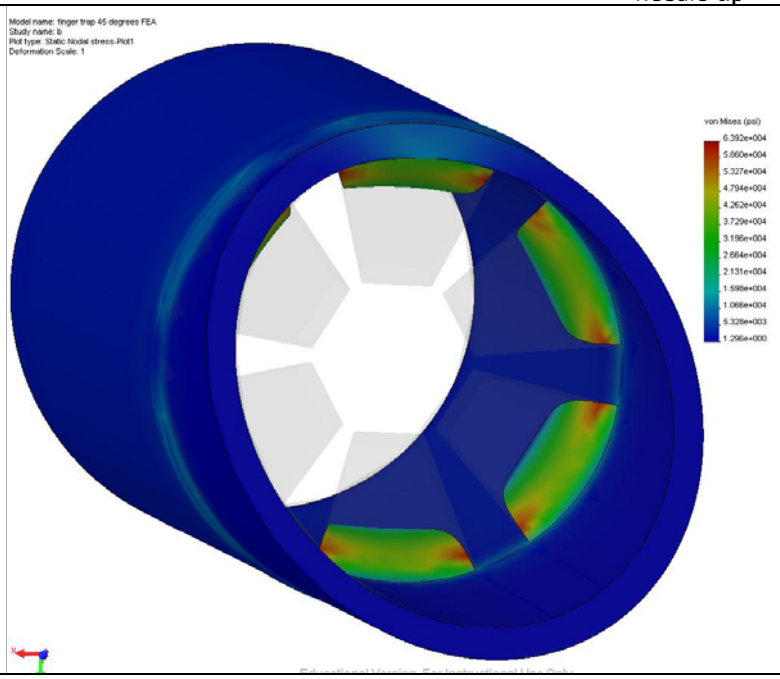

Figure 36: a) Leaflet Geometries that were tested using FEA, b) COSMOSWorks FEA of typical flexures showing yielding in red for a geometry without stress relief

Four variations on flexure shape were tested based on previous experience with cantilever shapes and stress relief improvements. These includes a tapered flexure section, a circular cutout at the base of the flexure, a flexure that lengthened up towards the needle tip, and flexure lengthened towards the inner section of the needle (Figure 36a). The wall-inclusive flexure that lengthened towards the needle tip performed ideally. As the tip penetrated into the tissue, both the walled and the internal components of the flexure deflected outwards; this was the optimal tissue capture mode. Upon extraction, the flexure closed appropriately, encapsulating the tissue as desired. Because the stress relief improves stress concentrations at the based of the flexure, it was also included as a

modification to the initial design. Finally, a taper was added only to the tip of the flexure that angled into the needle, as this section showed better deflection capabilities (Appendix F).

Given the analysis of Chapter 5 and the finite element estimates, a final drawing of the needle was produced so that manufacturing such a needle could be investigated. One such drawing is shown in Figure 37 with more detail available in Appendix G.

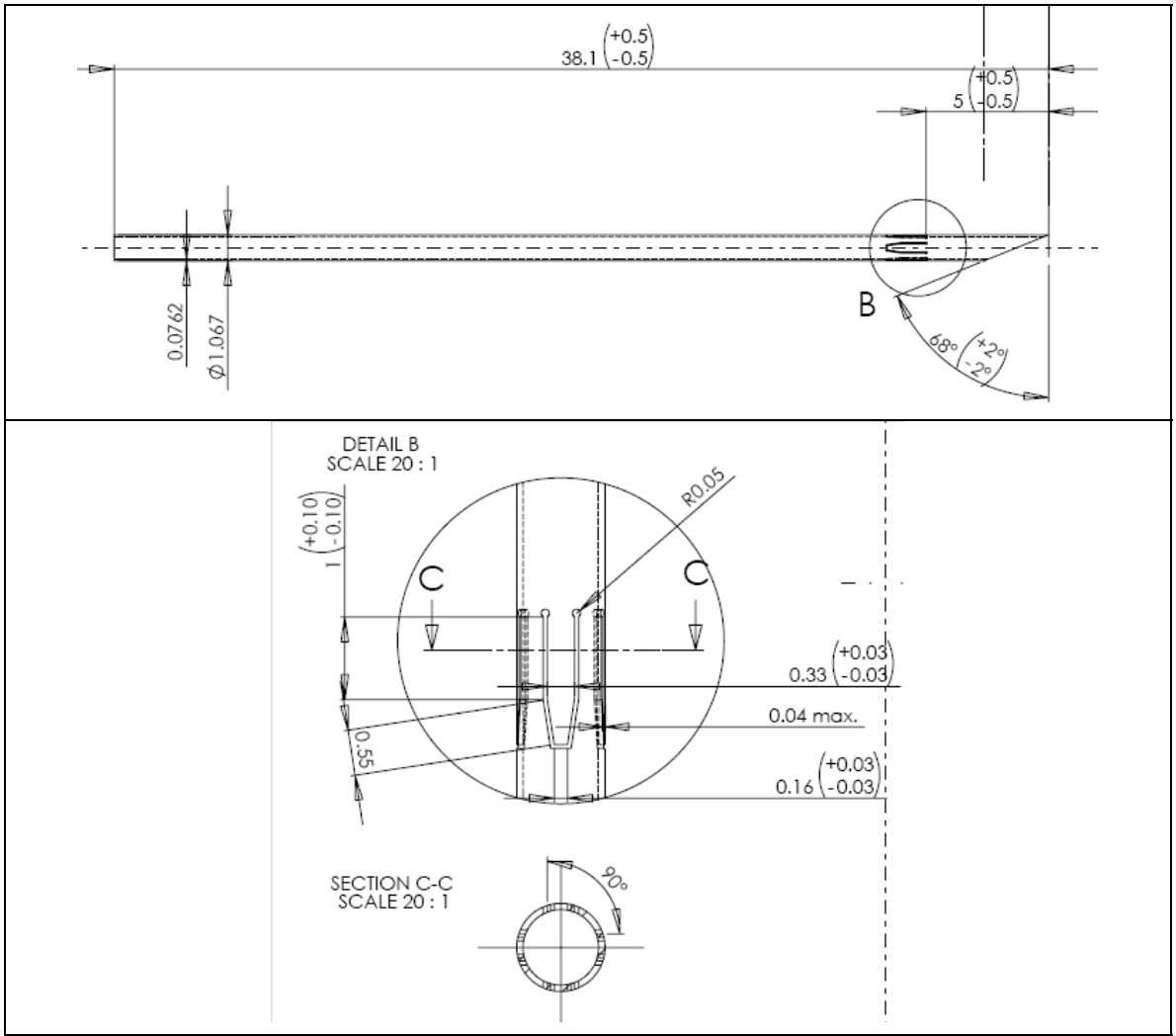

Figure 37: Drawing of final flexure concept after FEA analysis. (units in mm)

Chapter 7

1X SCALE NEEDLE MANUFACTURING PARAMETERS

Before going on to produce a full scale needle, issues related to manufacturing of a new needle design were investigated. This allowed the difficulties with integration of other needle components to be identified, along with challenges and limitations that could arise from the proposed changes. These issues include bending of the flexures to their initial angle and how to accomplish such a task given the largest dimension of just over one millimeter. It also involved determining how to manufacture the needle tip, as a separate component that could be added to a larger tube, or whether it should be cut into the existing design. It also involved testing several prototyping issues such as whether the bevel angle of a needle affected the piercing force, which would lead to failure of a prototype for reasons other than the added features.

7.1 Springback Compensation and Testing

Materials behave elastically (Hooke's Law applies) when stressed below their yield strength *Y*. However, when stressed beyond its yield strength, it no longer behaves elastically but is permanently deformed to some extent. This point on the stress-strain curve is where the initial linear slope begin The extent to which a metal recovers from an applied load is know as springback. This effect can be beneficial because it means

that small forces on an object to not necessarily permanently damage the material. However, it also means that the displacement that you apply to an object does not necessarily cause permanent deformation. As a common example, if you bend a playing card in half and then release it, the card is not necessarily bent as far back as you had initially hoped it would. This effect is also present in a metal flexure, which allows the cantilevered structure to be permanently bent with a large force, but to recover from the small forces in its use within a biopsy needle. The standard springback equation uses the initial bending radius R_i sheet thickness T, Young's Modulus E, and Yield Strength Y, to determine the final bending radius R_f.

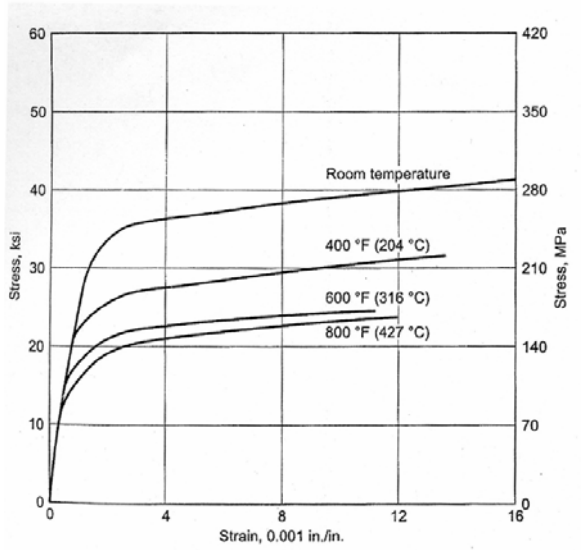

Figure 38: 304 Stainless steel stress-strain curves. Source Atlas of Stress and Strain

$$\frac{R_i}{R_f} = 4\left(\frac{R_i Y}{ET}\right)^3 - 3\left(\frac{R_i Y}{ET}\right) + 1 \qquad \text{Eq. } 16^{36}$$

assuming a constant arc length s, the final angle of the bend would be:

$$bend\_angle = \frac{360s}{2\pi R_f} \qquad \text{Eq. 17}$$

Bending flexures with a nominal thickness of 0.0762 mm (0.003 inches) and an overall length of 1.6mm required thinking of springback effects to ensure the desired

bend angle would result from a manufacturing step. Because of their thin structure, it was thought that the standard springback equation might underestimate the necessary initial bending radius. By this calculation, the flexures of the endoscopic biopsy needle tip would need to be bent at to 21.2 degrees to ensure a 15 degree bend.

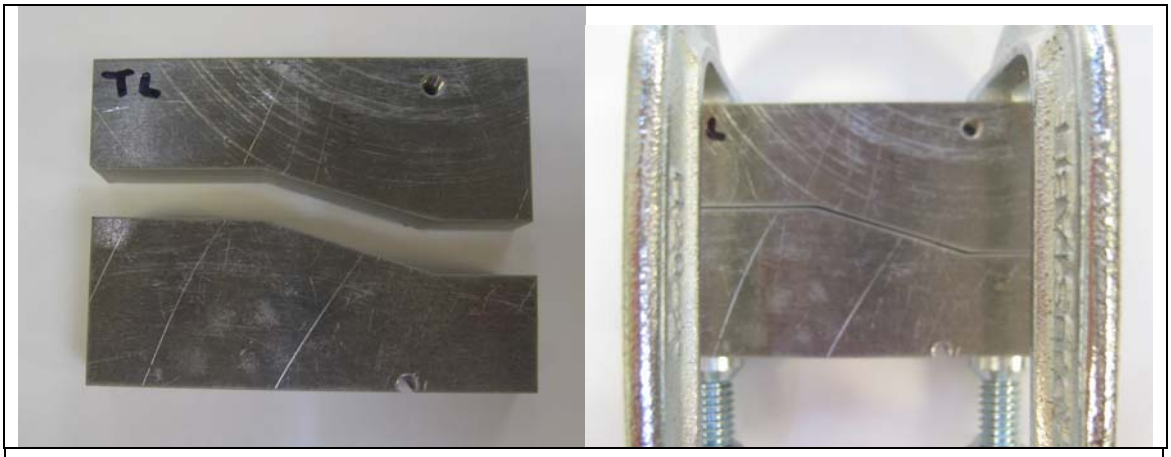

Figure 39: Bending die for flexure springback estimation.

To verify this equation for thin strips, a small die set with a 5mm radius of curvature was water jet for use on thin strips of 0.178mm (0.007in) 304 stainless steel. According to the above equation, these strips would need to be bent to an initial radius of 17.2 degrees to achieve a 15 degree final bend (Appendix H). Strips were pressed with a clamp into the die (Figure 39). The average angle of 13 degrees post-bend suggested that the above equation did in fact slightly underestimate the necessary bend (Figure 40). For this reason, a 22 degree die was used for the final prototype bend.

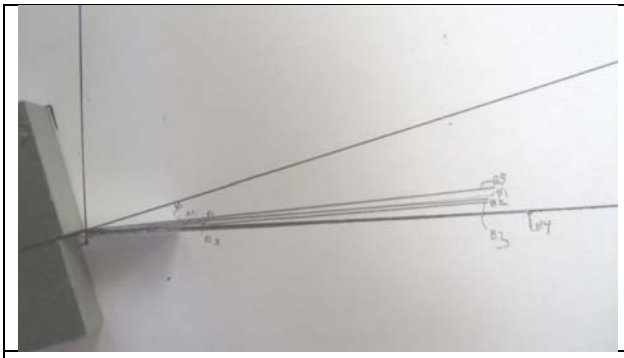

Sample	**Angle**
B1	12.5
B2	13.5
B3	13.0
B4	15.0
B5	11.5
Average	13.0

Figure 40: Springback samples of 0.178mm thickness 304 stainless steel showing average springback of 13 degrees from an initial 17.2 degree bend.

7.2 Needle Tip Integration with Bulk Needle Design

Following the design of internal flexures that could increase tissue retention, the issue of how to integrate this needle feature with a standard needle arose. Because of the manufacturing involved, it would be possible to create a separate needle tip that could later be attached to a longer tube section if such a process proved to be more manufacturable. Bench level experiments with crimping and threading of a 19-gauge hypodermic tube, tests of adhesives for medical products were conducted, and other methods of tube fitting connections were compared for their relative ease of manufacturing as well as how they would affect the use of a biopsy needle during tissue sampling. The connection methods were compared for their strength, reliability, how easily the tip could be removed to obtain a sample, and how easy the tip connection could be manufactured.

A crimp feature was seen as having an average connection strength, reliability, and removability rate of 3 (scale of 1 to 5 where 5 is a better rating) and to be easily manufactured with a one step hand crimping tool. Adhesives were tested and show to produce a strong joint, a safe connection, and easily removable interface. They would be slightly more difficult to produce than a crimp because a lap joint or sheath would need to be used in combination with the adhesive for a weld to be made. In addition a 2 part epoxy mix could waste material and take up valuable production time, while a cyanoacrylate adhesive may need a sanding treatment to guarantee proper surface wetting. A lap joint and swaging process to expand a needle tip over another tube was also considered. Unfortunately, this process would not be reliable without an adhesive or crimp to ensure the hypodermic tubing does not slip. Although snap fit or twist-lock tips would allow for easy removal, the manufacturing of such a feature would introduce complexity to the part and could become disconnected when bent through an endoscope.

The simplest solution from a manufacturing standpoint would be to have no connection at all; and this method was also considered. Cutting the needle tip features from an existing needle (no separation) was seen as being the strongest connection, because the only failure mode was the weakening of the needle material. This would eliminate failure at a joint or of the adhesive within a joint. It was also seen as the easiest to manufacture, since the part count was lower and involved fewer tube cuts. Although handling the entire needle length may be cumbersome when cutting only the front few centimeters of the needle tip, it was decided that this situation would not be more difficult to handle since a custom jig would need to be made to accurately cut the features regardless of the tip length. A needle with no separation could produce very poor samples if one were forced to remove the sample through the entire needle length, but may produce a better sample if it were combined with a cutoff tool. This would allow the needle tip to be removed by a doctor once a sample has been taken without introducing additional complexity to the needle itself. After comparing the all of the proposed integration strategies, the integrated needle tip with no separation from the rest of the needle length was chosen as the preferred manufacturing method. The secondary method of producing a tip that could be joined using and adhesive and lap joint was considered a viable option for prototyping purposes.

Table 6: Needle tip integration strategies

Connection Types	**Strength**	**Reliability/Safety**	**Removable**	**Manufacturability**	**TOTAL**
Crimp	3	3	3	5	14 *
Adhesive	4	4	3	4	15 **
Thread	3	3	4	2	12
Lap / Swage	4	3	2	5	14 *
No separation	5	5	3	5	18 ***
Snap fit	2	2	4	2	10
Twist-lock	2	2	4	2	10

*** manufacturing step (expensive for prototype)
** close alternatives (good for prototyping, or if costs of full needle cut too high)
* adhesive can combine with either of the prototyping methods

7.3 Bevel Angle Sensitivity

Figure 41: Bevel angle of needle tip.

Figure 42: Test setup of beveled needle piercing liver tissue using a TA.XTPlus Texture Analyzer.

Before recommending a needle tip for production, it was necessary to determine the appropriate bevel angle for the needle tip and whether the angle had any effect on cutting ability of the needle. After researching the needle options available from several manufacturers,[17,37] typical angles varied from 15 degrees to 30 degrees, with custom shapes available. Because it was assumed that tissue acquisition was not affected by the bevel, a standard straight angle was varied and puncture force was measured. Two common bevel angles 22 degrees and 30 degrees were inserted into a sample of calf liver (store bought) and the first puncture force was measured using the same TA.XTPlus mentioned earlier. With target displacements of 15mm, eight samples of each needle were used to pierce the liver.

This puncture did not include the capsular tissue surrounding the liver but pierced the bulk tissue. This setup was meant to prevent motion of the sample relative to its container, which would have affected the measurements by displacing tissue without actually piercing.

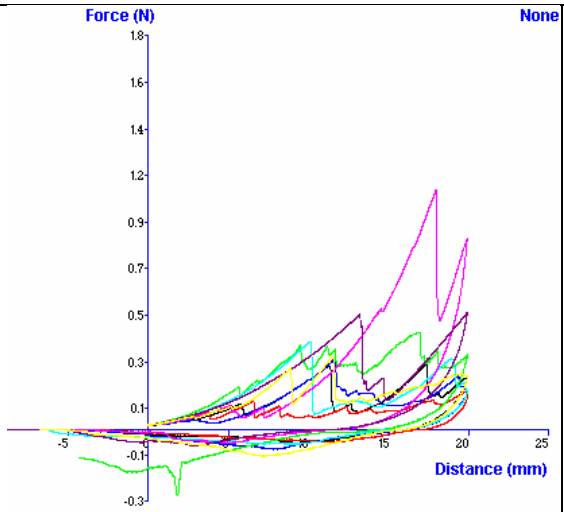

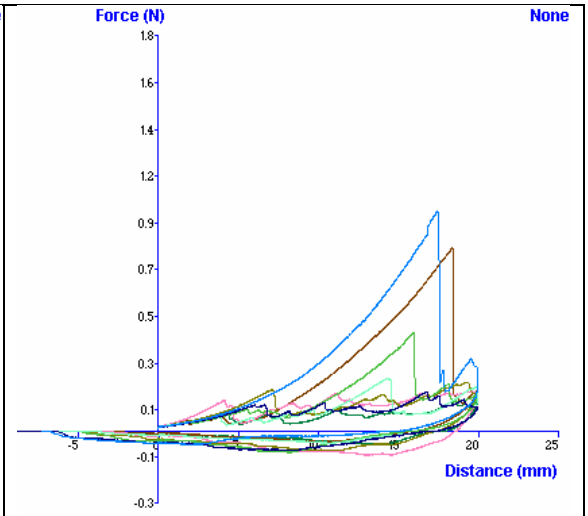

Needle #	Bevel Angle	Puncture Force (N)
1	22	0.30
2	22	0.32
3	22	0.14
4	22	0.38
5	22	0.40
6	22	0.11
7	22	0.53
8	22	0.28

Average Puncture Force (N)	Standard Deviation
0.31	0.14

Needle #	Bevel Angle	Puncture Force (N)
9	30	0.09
10	30	0.84
11	30	0.14
12	30	0.19
13	30	0.45
14	30	0.07
15	30	0.12
16	30	1.00

Average Puncture Force (N)	Standard Deviation
0.36	0.37

Figure 43:Puncture force of 22-degree and 30-degree bevel needle blanks

After finding the peak piercing force for each of eight sample needles the average puncture force for the 22 degree needle was 0.31N with a standard deviation of 0.14N. The 30 degree bevel needle had an average puncture force of 0.36N with a standard deviation of 0.37N. This data suggested that there was no significant difference in puncture force between the two needles. Assuming the needle tip only affects puncture force and does not affect tissue acquisition or tissue retention, a simple bevel angle could be ground for manufacturing and prototyping purposes. It was decided that a 22 degree bevel would be used for future needle prototypes.

7.4 1x Scale Needle Prototype Manufacturing

To gain an understanding of how well FEA analysis and scale needle prototypes could approximate a 1x scale needle, prototypes of the actual needle tip were created using a grinding process as well as a laser cutting operation to produce internal flexures. The flexures were bent using a ground insert to help guide the bend angle. Below is an explanation of the steps that were taken to produce such a part. This process sheds light on the relative ease of producing the needle, and also revealed manufacturing issues that may not have been noticed otherwise.

7.4.2 Production of Ground Needle Tips

Using 1.06mm outer diameter (19 Gauge) 304 stainless steel tubes with a wall thickness of 0.0762mm (0.003in), lengths of rod approximately 50mm long were cut from drawn tubing using standard wire cutters. Each section of tube was placed in a pin vice with approximately 8mm of material cantilevered out of the vice. The pin vice itself was then fastened into a standard vice, which prevented the pin vice and stainless steel tube from rotating. This configuration allowed a cylindrical tube to be positioned using a flat surface as a guide. Because previous tests showed no significant difference in puncture force between 22 degree and 30 degree bevel angles, this accuracy of clamping was acceptable for grinding.

Once clamped, the vice and needle assembly was located on the flat base of a grinding tool and the relative angle of the needle to the grinding wheel was set using an integrated protractor on the grinding tool. Grinding of the needle tip was straightforward as the main concerns were: to maintain a consistent grinding angle, not to bend the rod by forcing the rod into the grinding wheel, and to remove all of the tube on the tip that may have been stressed or deformed by cutting with wire cutters. To grind off the back end of the needle, calipers were used to approximate the length of the needle to 38.1mm (1.5”).

The sharpened needle was then placed in a Wilton cutoff tool to cut the needle to its final length, which was accurate to within 1mm of the desired length.

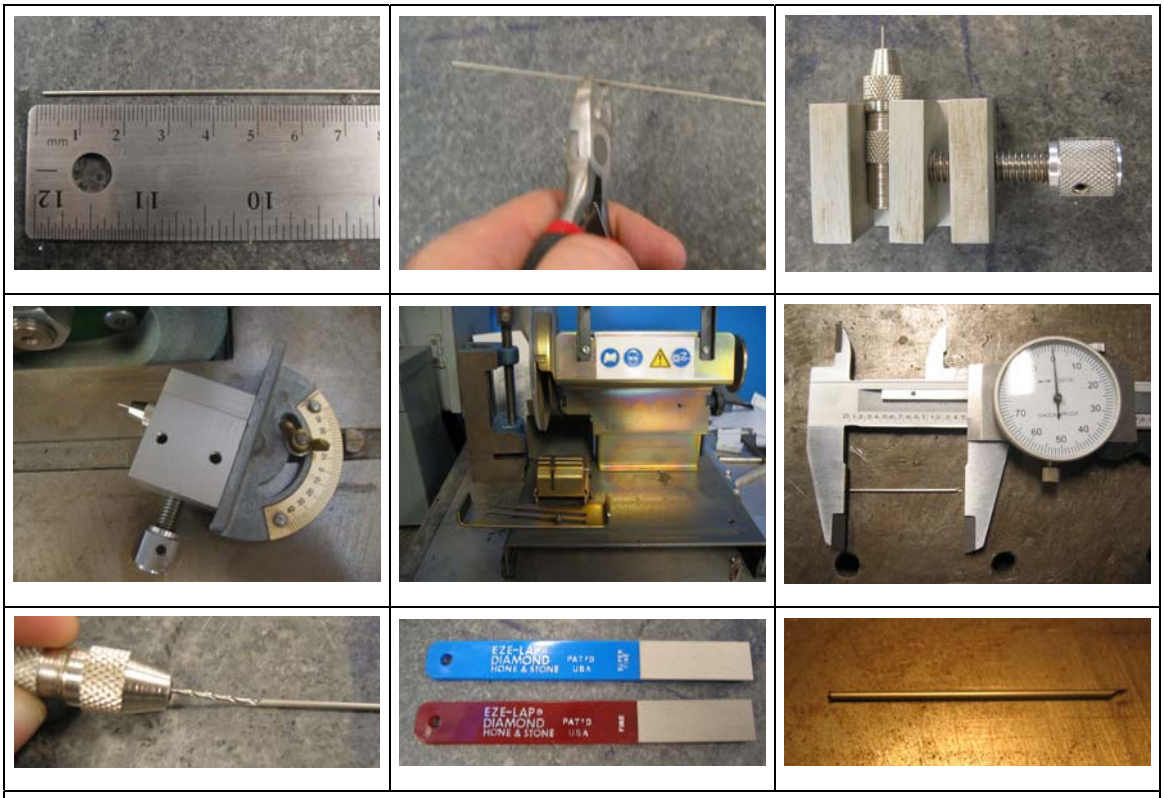

Figure 44: Needle Tip Grinding Process (Left to Right, Top to Bottom) Measure length, Rough cut, Clamp using vice, Grind bevel, Grind flat end, Measure length, De-burr, Hone tip, and Resulting needle.

Once cut to the approximate length, finishing of the needle was required to ensure sharpness that was similar to mass-produced needles. Each needle was deburred using a 68 drill bit and was filed to its final length with a fine grit honing stone. The needle tip was sharpened using a superfine 1200 grit honing stone. This process is summarized in Figure 44 and an image of the tip surface after production is shown in Figure 45.

Figure 45: Image of needle tip prototype after processing.

7.4.2 Laser Cutting of Flexures into the Needle Wall

Once a blank needle tip was produced as a prototype, the features of the needle had to be produced. To create such a small feature into a part, where both the thickness of the flexure and the thickness of the remaining needle were significant, a laser cutting process was chosen. Laser cutting of stainless steel can usually be accomplished by either a CO_2 or an Nd:YAG laser[38]. The laser cutting process allowed a kerf thickness of 0.05mm or smaller, with only minimal damage to the surrounding metal. Some oxidation was observed on the cut, but this result could easily be remedied by using an electropolishing

or passivation procedure following the cutting step. Because the exact amount of metal that would be removed could not be quoted by a vendor, this step was left as an item that could be studied once the performance of non-electropolished flexures was known, and so that the dimensions of the flexures was not altered in an uncontrolled way. Images of flexure cut into the needle wall are shown in Figure 46. Once the flexures were cut into the needle wall, the were easily bent into the desired shape using a 22 degree insert that, with springback of the metal, would produce the desired 15 degree bend angle.

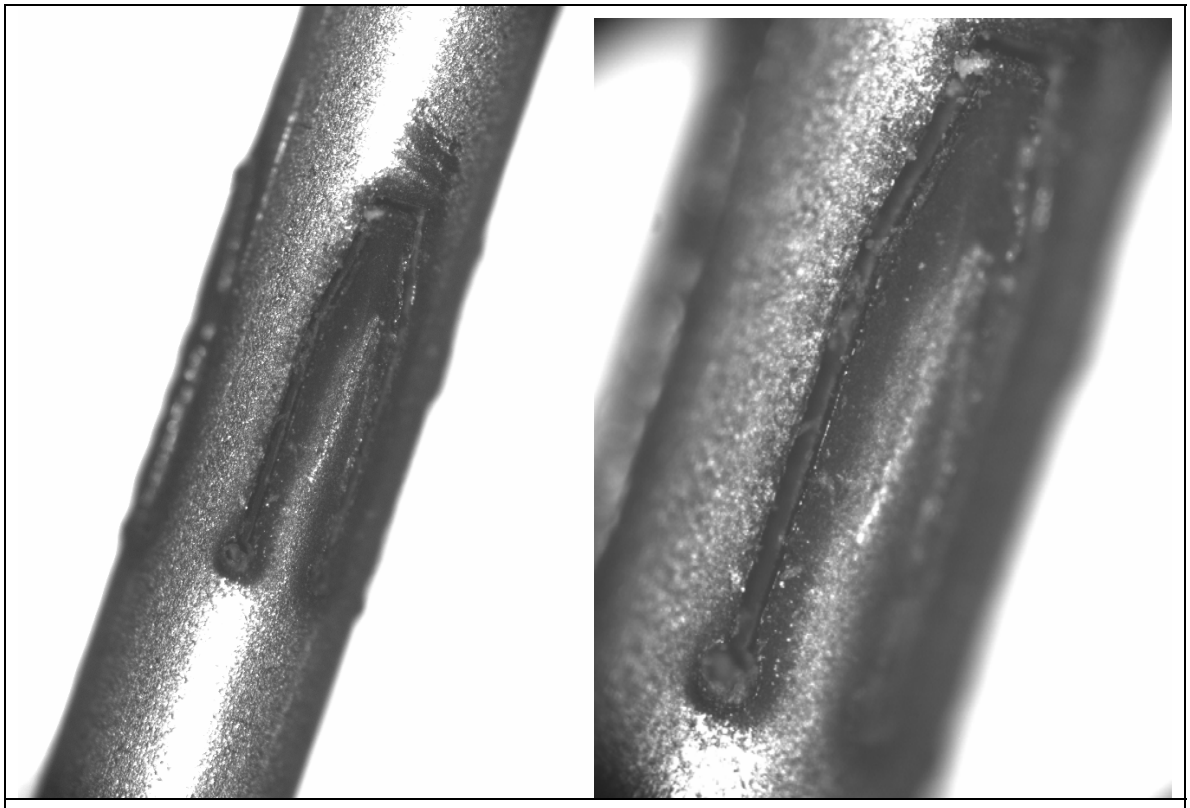

Figure 46: Laser cut features on a 19gauge (1.06mm) needle with a kerf width of 0.05mm.

Chapter 8

DISCUSSION CONCLUSIONS AND FUTURE WORK

8.1 Positive Developments in the Design of an Improved Endoscopic Biopsy Needle

Several patterns emerged when comparing the data collected from scale prototypes and through manufacturing of a 1 x prototype. Flexural members in the 10x experiments produced a larger sample mass than a wedge design and an extended wedge with the same feature angle. When comparing needle insertion forces on the 10x scale using a gelatin phantom, the flexural design exhibited a lower resistance when inserted and a higher resistance when extracted from gelatin than wedge shaped needles. This could be explained be the deflection of the flexures when the needle is penetrated into a sample. As a needle is inserted, the flexures are able to deform and allow tissue through, whereas a wedge design cannot. When the needle is extracted, a flexural needle can use the principle of self help to deform and close off the tip of the needle, capturing a sample inside the needle. A wedge shape, although biased in one direction, cannot react to an increased force with an increased wedge angle. These results suggest that flexural ability of internal features is beneficial for tissue retention.

A relationship between the angles of flexures in the needle was also observed in 10x scale needle prototypes, where a lower angle flexure of 15 degrees was seen to produce

the most tissue when compared to 30 degree, 45 degree, and 60 degree features for both wedge shapes and for the flexural design. This pattern could be explained by the fact that even a small amount of entrance resistance can prevent a sample from entering the needle. In addition, only a small amount of additional resistance is needed to retain a sample. If an inner feature has too high a resistance upon entrance, it can be detrimental to sampling by limiting the amount of tissue that passes by the flexures. Therefore, even if these features are able to produce a strong retention force, there is very little for the features to retain.

8.2 Limitations of the Current Design and Testing of 1x Scale Prototypes

By manufacturing a 1x needle prototype that was optimized using finite element analysis to prevent buckling and to balance flexure motion during needle insertion and removal, it was shown that flexures could be produced on an actual needle. Flexural features can be successfully produced in the wall of a stainless steel needle with the precision necessary for manufacturing using basic grinding and laser cutting processes. These flexures were deformed to 15 degrees within the needle wall and could were able to deform without evidence of failure such as brittle fracture, which would be a significant risk to a patient.

Compared to the initial assumption that flexures can use the principle of self help to retain tissue samples, the 10x scale needles verify this assumption. The suggestion that these features can be produced without failure was also supported by manufacturing of scale needles. Still there are several issues with the resulting needle that did not perform as expected.

Following the manufacturing process of 1x scale needles, both featureless needles and needles with internal flexures were tested on store bought liver tissue. Both the original hollow needle and the flexural needle failed to retain a core sample when the needle was

measured before and after puncture. For eight puncture tests of the featureless needle and 24 punctures of flexural needles, this was an unexpected result. Observations of the tests showed that retention of a sample was not the issue, but that a core of tissue did not enter the needle to begin with. It was thought that perhaps store-bought liver tissue was significantly different from live tissue and the gelatin that was used frequently for sampling such that it prevents coring. However, the same procedure was tested with a gelatin phantom, which because of it lack of cellular structure would be easier to core, also produced no significant core samples for featureless needles of flexural needles.

It should be stressed that because even a featureless needle failed to produce a core, the failure should not be attributed to the flexural design. The failure of 1x scale needles not to retain a core, but to acquire a core sample revealed a difference between the initial assumption that the needle tip was effective when coring and the observed coring failure. While 10x scale needle tips were effective at coring and allowed the flexures to be tested, on the 1x scale, this did not seem to be the case. For a flexural needle to be tested and compared to a featureless needle on a 1x scale, the tip of the needle would have to be altered first. For retention of a sample to be tested, issues with acquisition would have to be remedied.

Research into coring needles other than those used for endoscopic biopsy revealed a number of alternatives to the standard beveled tip. Currently, it is hypothesized that the bevel of the needle, which normally acts as a wedge to pierce through tissue, also causes tissue to slide past the plane of the needle bevel without coring. By making the simple change of a different tip shape, possibly on of the existing serrated shaped used for bone biopsy, or the blunt cone shape used in percutaneous biopsy, the acquisition of needle tissue could be improved. This design change could then allow a more successful test of flexural needles using liver tissue and 1x scale prototypes.

While data acquired from tests of the flexural needle biopsy suggest that internal flexures can improve tissue sampling reliability, this claim cannot be fully substantiated

until tested on the 1x scale with live tissue. Because differences in tissue acquisition were observed with different needle scales, future tests should continue using 1x scale prototypes. To test the flexural concept further would require adjustments to the needle tip so that tissue enters the needle and the flexures could engage a sample.

8.3 Conclusion

By researching the function of a biopsy needle and limitations of current designs, a series of design strategies were identified that could improve tissue retention within a hollow endoscopic biopsy needle. Needle strategies were tested using gelatin phantoms and scale prototypes to develop a concept that retains tissue using flexural elements within a hollow coring needle. Testing the parameters of a flexural biopsy needle and finite element analysis les to the design of a prototype with four flexures angled at 15 degrees into the needle wall. To maximize flexure deflection while remaining below the yield strength of stainless steel, the flexures were extended to include a portion of the needle wall as its length, with the final 0.6mm of a 1.6mm flexure being tapered and bent into the hollow needle. Following successful results of 10x scale stereolithographed needles, manufacturing of 1x scale stainless steel needles using grinding and laser cutting produced high quality prototypes. These 1x scale prototypes were able to pierce tissue, and flexures were responsive to probing. However, testing of 1x scale flexures to retain samples was prevented by the inability of the needle's beveled tip to core a sample.

Producing a scale prototype on the 1x scale, while showing a flexural design was able to be made with relative ease, identified an issue with tissue acquisition that prevented 1x scale needles from being tested. Addressing this issue by altering the tip bevel to another coring shape would be the first point of improvement to the current flexural design.

8.4 Future Work

While significant progress has been made to improve tissue retention capability of endoscopic biopsy needles using flexural elements, there remain several key points that

should be addressed before proceeding with marketing of such a design. The first point to address would be to compare the coring ability of needlepoints, using the standard bevel points as a reference that a design must improve upon. Such a test would compare tissue mass of a 1x needle while varying only the shape of the needle point. After identifying the needle point that acquires the most tissue, this needle point should be used to test the tissue retention ability of a flexural needle compared to a needle with no internal features.

There are currently several available needle point styles available from custom manufacturers that differ from the standard beveled needle tip which should be tested for endoscopic biopsy. A cone bipsy needle tip, Gardner type bone marrow biopsy tip, Silverman dual pointed tip, or a hybrid design that combines one of these ideas with the standard would be a promising (Figure 47).

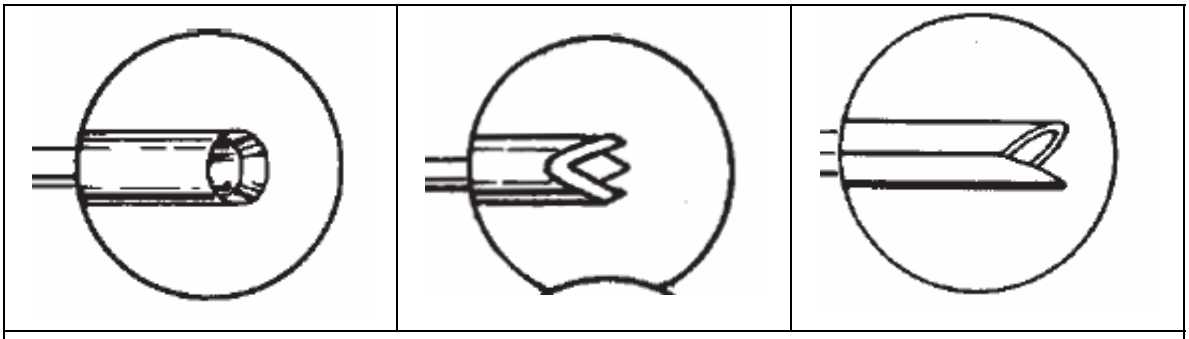

Figure 47: Alternate needle tips that could be used in endoscopic needle design (left) cone biopsy needle with beveled inner surface, (center) gardner type needle with multiple points, (right) Silverman dual-point tip. Source: Popper and Sons

Because of the differences in coring on the 10x and 1x scale, final comparisons should be tested using 1x scale stainless steel needles and liver from recently sacrificed animal. If results from such a test produce positive results, testing of a full needle and complete endoscopic procedure in an operating room setting using animal models. It is the aim of the author to continue this work until needle prototypes can be shown to produce improved tissue sampling results in animal trials. A patent is currently pending on these new biopsy needle designs.

Appendix A

PIERCING FORCE OF A 1X STAINLESS STEEL NEEDLE WITH 30-DEGREE BEVEL

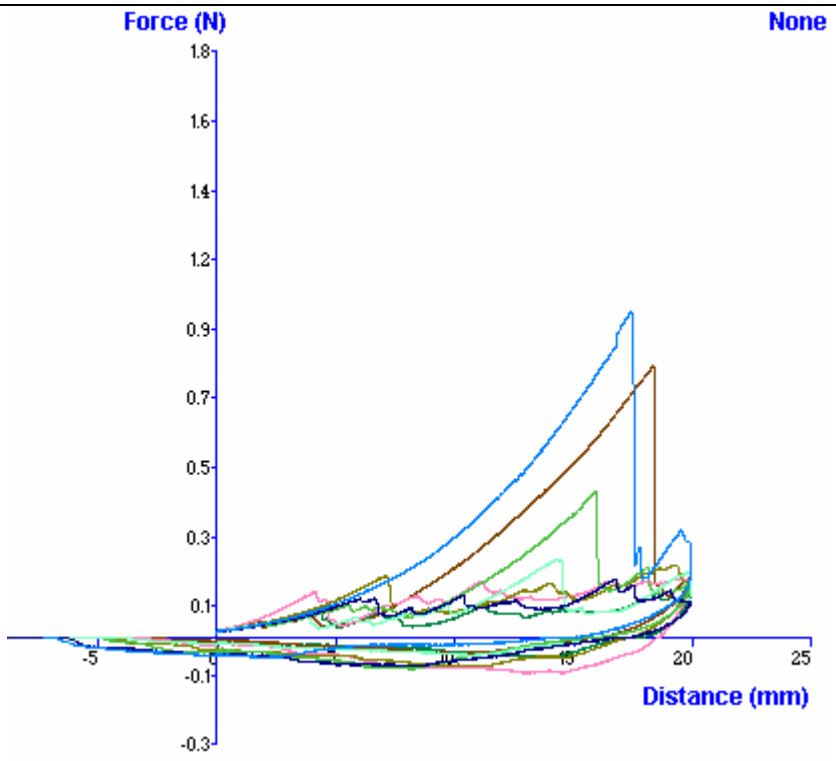

Puncture force of beveled needle tip, where the initial drop resulting from tissue puncture was used to determine tissue cutting forces, as well as whether or not bevel angle affects tissue puncture forces.

Appendix B

NEEDLE CORING STRATEGIES FROM BRAINSTORMING SESSIONS

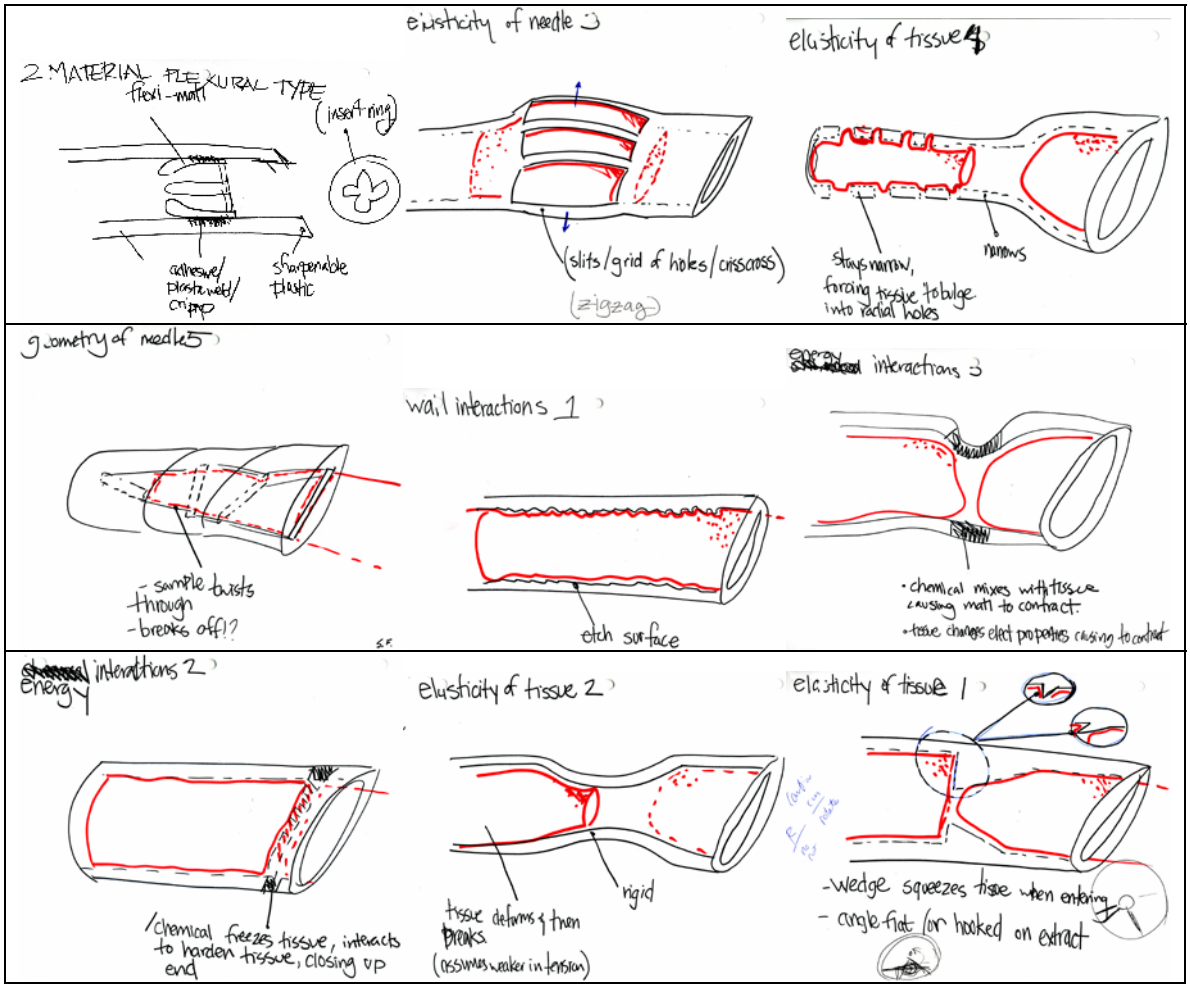

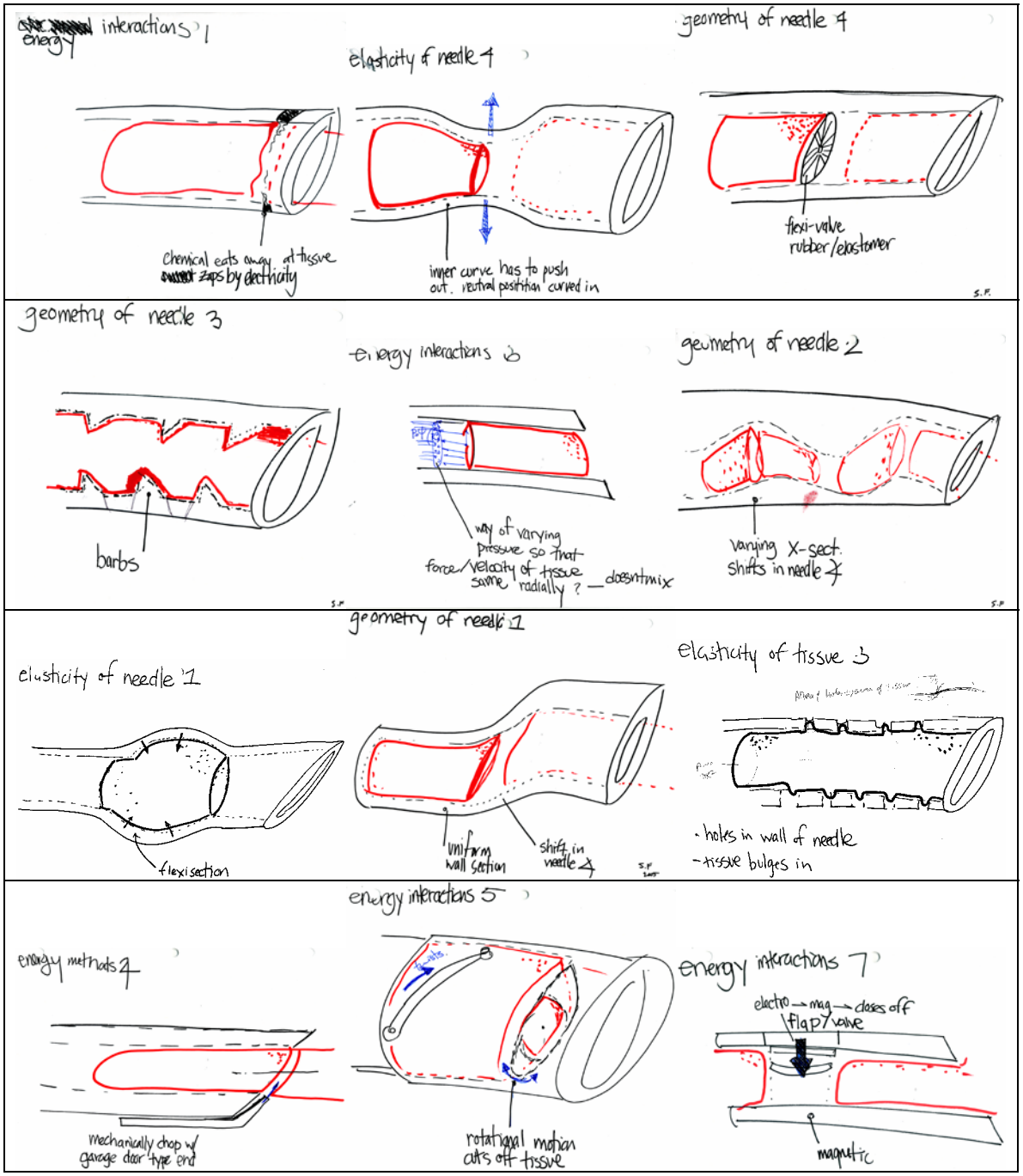
energy interactions 1
chemical eats away at tissue
zaps by electricity
elasticity of needle 4
inner curve has to push out. neutral position curved in
geometry of needle 4
flexi-valve
rubber/elastomer
geometry of needle 3
barbs
energy interactions 6
way of varying pressure so that force/velocity of tissue same radially ? doesn't mix
geometry of needle 2
varying X-sect. shifts in needle
elasticity of needle 1
flexisection
geometry of needle 1
uniform wall section
shift in needle
elasticity of tissue 3
- holes in wall of needle
- tissue bulges in
energy methods 2
mechanically chop w/ garage door type end
energy interactions 5
rotational motion cuts off tissue
energy interactions 7
electro → mag → closes off flap/valve
magnetic

Appendix C

COMPARISON OF CUTTING STRATEGIES AND CONCEPTS

Qualities	Weight	Current Side Cut	Current End Cut	3 Pronged Tweezers	Finger Trap	Barbs
Success Rate	10	2	3	4	5	5
Sample Quality	10	3	3	4	4	3
Manufactionabilty	7	3	3	3	4	3
Ease of Getting Sample	6	4	4	3	5	5
Ease of Removing Sample	3	3	3	2	3	2
Multiple Samples	5	1	3	1	4	4
Total multiplied by weight	41	109	129	130	177	157

Appendix D

MATLAB SCRIPT TO ALTER NEEDLE PARAMETERS

(Working file. May have been changed from original parameters)

```
%Flexing of Needle
% overestimates slightly because does not take into account the flexing of
% that the deflection of the needle changes the applied force as it opens.

n=4; %number of flexures
F=5; %Total Force applied to needle (Nexwtons)
Fperflex=F/n; % Force per flexure
Fnormal=Fperflex*cos(pi/12); %normal force to flexure
E=193*10^9; %Youngs Modulus of 304 Stainless Steel
wallthickness_in=0.003; %wall thickness in inches
wallthickness_mm=0.003*25.4 %wall thickness in mm
innerwall_diameter_in=(0.042-2*wallthickness_in); %dimensions for 19G ultrathinwall needle
innerwall_diameter_mm=innerwall_diameter_in*25.4
inner_radius_mm=innerwall_diameter_mm/2;
flexurearc=38%what part of the circumference of the needle is each flexure in degrees
finding_b=(innerwall_diameter_in+wallthickness_in)*pi*(flexurearc/360)*25.4; %finds the flexure
width from the median diameter
%and fraction of the circumference



b_mm=finding_b  %width of flexure using or insert default .275 (mm)
b=b_mm/1000;
h=0.003*2.54/100; %flexure thickness (meters)
I=(b*h^3)/12; %bending moment of flexure
L=.0005; %flexure length (meters)
d=Fnormal*L^3/(E*I*8); %tip deflection for distributed load  (in Roarks L^4, but this fits better with
solidworks estimates)
d_mm=d*1000 %deflection in mm
initial_gap_mm=L*sin(pi/12)*1000


percent_of_innerrad=initial_gap_mm/inner_radius_mm*100 %what percent of the radius is the
flexure occupying
tip_to_wall_dist_mm=initial_gap_mm-d_mm %distance of the tip to the inner wall of the needle
(approx)
```

Appendix E

MATERIAL PROPERTIES LISTED FOR T304 STAINLESS STEEL[39]

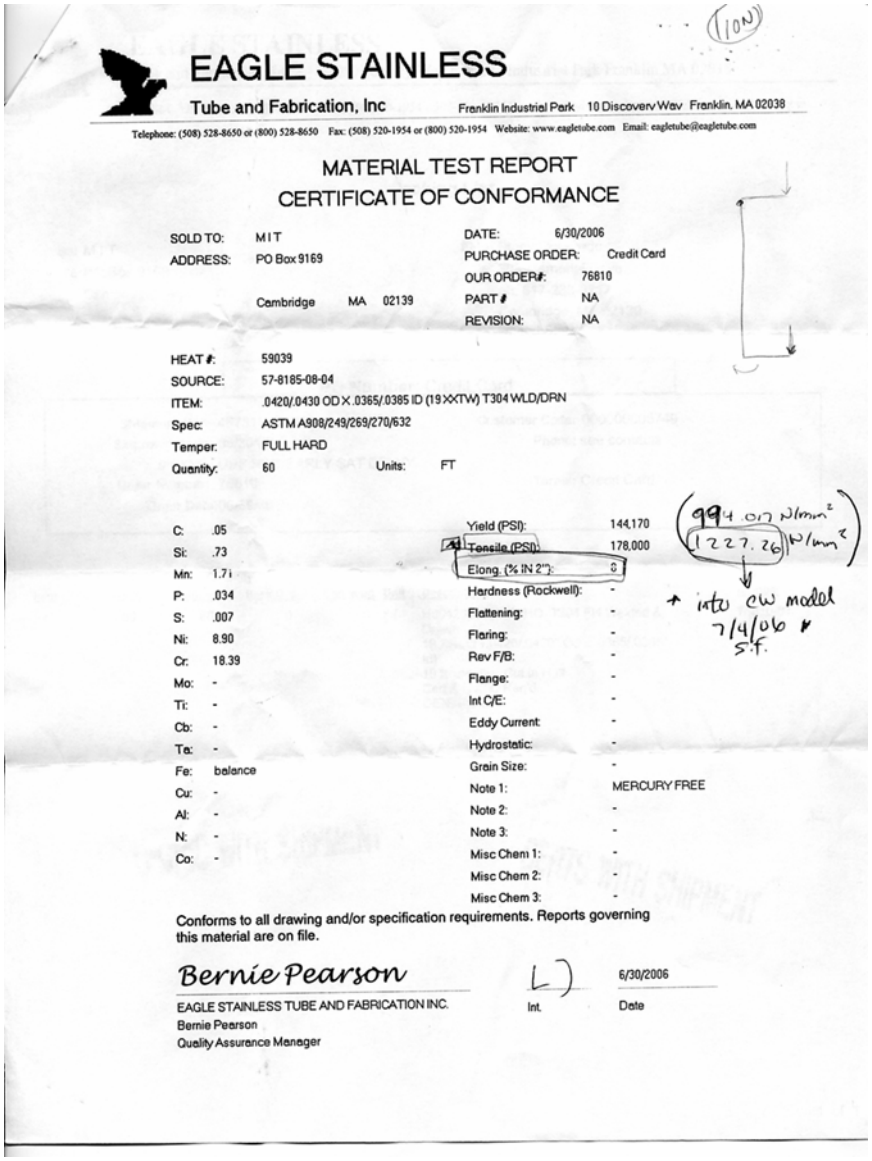

EAGLE STAINLESS

Tube and Fabrication, Inc Franklin Industrial Park 10 Discovery Way Franklin, MA 02038

Telephone: (508) 528-8650 or (800) 528-8650 Fax: (508) 520-1954 or (800) 520-1954 Website: www.eagletube.com Email: eagletube@eagletube.com

MATERIAL TEST REPORT
CERTIFICATE OF CONFORMANCE

SOLD TO: MIT
ADDRESS: PO Box 9169
Cambridge MA 02139

DATE: 6/30/2006
PURCHASE ORDER: Credit Card
OUR ORDER#: 76810
PART #: NA
REVISION: NA

HEAT #: 59039
SOURCE: 57-8185-08-04
ITEM: .0420/.0430 OD X .0365/.0385 ID (19 XXTW) T304 WLD/DRN
Spec: ASTM A908/249/269/270/632
Temper: FULL HARD
Quantity: 60 Units: FT

C:	.05
Si:	.73
Mn:	1.7 i
P:	.034
S:	.007
Ni:	8.90
Cr:	18.39
Mo:	-
Ti:	-
Cb:	-
Ta:	-
Fe:	balance
Cu:	-
Al:	-
N:	-
Co:	-

Yield (PSI):	144,170
Tensile (PSI):	178,000
Elong. (% IN 2"):	0
Hardness (Rockwell):	-
Flattening:	-
Flaring:	-
Rev F/B:	-
Flange:	-
Int C/E:	-
Eddy Current:	-
Hydrostatic:	-
Grain Size:	-
Note 1:	MERCURY FREE
Note 2:	-
Note 3:	-
Misc Chem 1:	-
Misc Chem 2:	-
Misc Chem 3:	-

994.07 N/mm² (1227.26 N/mm²) → into CW model 7/4/06 * S.F.

Conforms to all drawing and/or specification requirements. Reports governing this material are on file.

Bernie Pearson Int. 6/30/2006

EAGLE STAINLESS TUBE AND FABRICATION INC.
Bernie Pearson
Quality Assurance Manager

Appendix F

DEFLECTION CAPABILITIES OF NEEDLE

order	Force Total (N)	# Flexures	Prebend Angle	Flexure Width	Flexure Length (mm)		Tip Deflection	Max Stress		Matlab deflection est
1	5	4	15	0.1696	0.75		0.0424	2.83E+09	too high	0.0531
2	5	4	15	0.1696	1		0.08	3.41E+09	too high-	0.1258
3	5	4	15	0.2161	0.75		0.0327	2.38E+09	too high	0.0414
4	5	4	15	0.2593	0.75		0.0274	2.01E+09		0.0345
5	5	4	15	0.3026	0.75		0.0216	1.42E+09		0.0296
	* after five tries ran buckling with 35 degree (.2593 and find that still have 23.2 N max buckling load... about 2.3k or 5lbs... about max I would give)									
	*let width equal approx 30-35 degree arc.2593-.3026mm									
	adjust length for deflectionby moving up into the needle shaft, which should help with stress a bit									
	**5N is a high force, that the flexures will probably not see, but thought to start high so as the parameters are narrowed down at first, will work will lower forces, and can relax them later									
	Force Total (N)	# Flexures	Prebend Angle	Flexure Width	Flexure Length (mm)	Top Flexure Length	Tip Deflection	Max Stress		
6	5	4	15	0.26	0.9	0.5		2.24E+09		
7	5	4	15	0.26	0.9	0.75		2.22E+09		
8	5	4	15	0.26	0.9	1		2.19E+09		
decent top length...doesn't do much to help with stress conc.										
now vary flexure length										
9	5	4	15	0.2593	0.75	1		2.00E+09		
10	5	4	15	0.3026	0.6	1		1.51E+09		
put the taper on the inner part				30 degree of wall						
11	5	4	15	0.3026	0.6	1		1.40E+09	tapered	
12	5	4	15	0.3026	0.6	0.75		1.42E+09	tapered	
				38degree of wall						
13	5	4	15	0.3285	0.6	0.75		1.28E+09	tapered	
14	5	4	15	0.3285	0.5	0.75			taper from .18 to .15	
Now Looking at Realistic Forces ~1N-2N total to adjust overall length										
15	1	4	15	0.3285	0.5	0.75	0.0099	2.30E+08	tapered	
16	1	4	15	0.3285	0.6	0.75	0.0125	2.54E+08	tapered	
17	1	4	15	0.3285	0.6	1	0.0166	2.52E+08	tapered	
18	2	4	15	0.3285	0.6	1	0.033	5.81E+08	tapered	
Closing Forces after for this part to look at closing deflections										
19	1	4	15	0.3285	0.6	1	0.0238	3.47E+08	tapered	
20	2	4	15	0.3285	0.6	1	0.048	6.95E+08	tapered	
21	1	4	15	0.3026	0.6	1	0.0265	3.74E+08	tapered	
22	2	4	15	0.3026	0.6	1	0.053	7.48E+08	tapered	
This last iteration is below the yield with 2 Newtons applied and still has a decent amount of deflection at the tip.										

Appendix G

DRAWINGS FOR FINAL FLEXURAL BIOPSY NEEDLE DESIGN

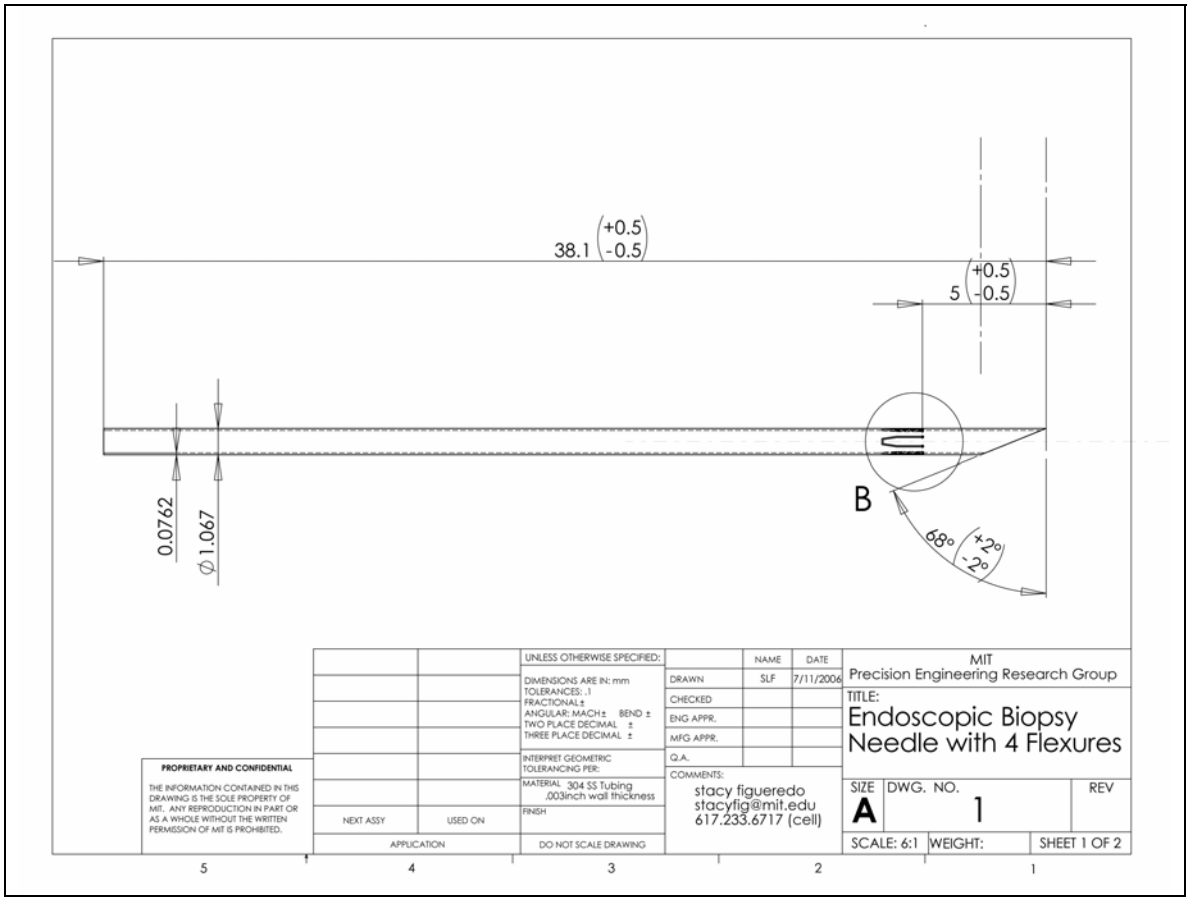

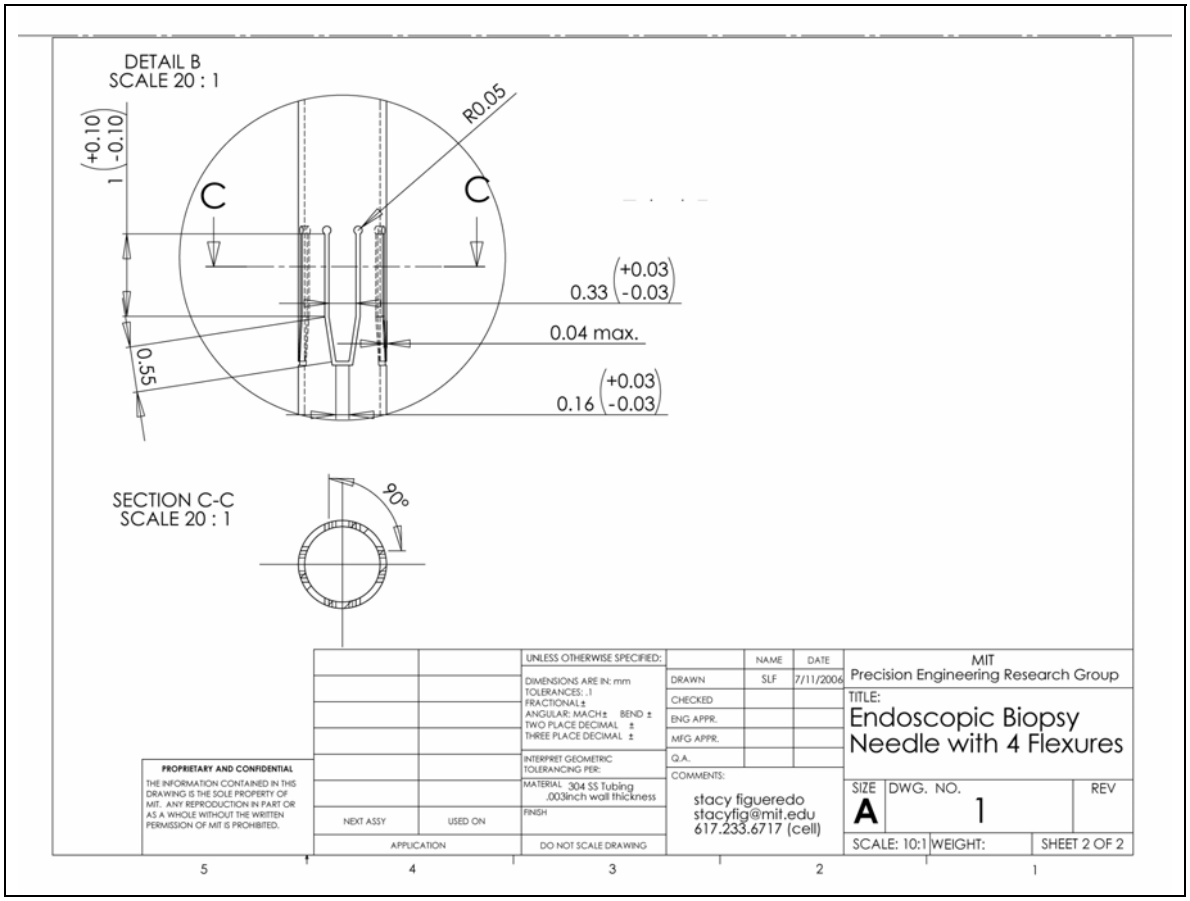
DETAIL B
SCALE 20 : 1
R0.05
(+0.10 -0.10)
1
C
C
0.33 (+0.03 -0.03)
0.04 max.
0.55
0.16 (+0.03 -0.03)
SECTION C-C
SCALE 20 : 1
90°
UNLESS OTHERWISE SPECIFIED:
DIMENSIONS ARE IN: mm
TOLERANCES: .1
FRACTIONAL ±
ANGULAR: MACH ± BEND ±
TWO PLACE DECIMAL ±
THREE PLACE DECIMAL ±
INTERPRET GEOMETRIC TOLERANCING PER:
MATERIAL 304 SS Tubing .003inch wall thickness
FINISH
NEXT ASSY
USED ON
APPLICATION
DO NOT SCALE DRAWING
NAME
DATE
DRAWN
SLF
7/11/2006
CHECKED
ENG APPR.
MFG APPR.
Q.A.
COMMENTS:
stacy figueredo
stacyfig@mit.edu
617.233.6717 (cell)
PROPRIETARY AND CONFIDENTIAL
THE INFORMATION CONTAINED IN THIS DRAWING IS THE SOLE PROPERTY OF MIT. ANY REPRODUCTION IN PART OR AS A WHOLE WITHOUT THE WRITTEN PERMISSION OF MIT IS PROHIBITED.
MIT
Precision Engineering Research Group
TITLE:
Endoscopic Biopsy Needle with 4 Flexures
SIZE A
DWG. NO. 1
REV
SCALE: 10:1
WEIGHT:
SHEET 2 OF 2
5
4
3
2
1

Appendix H

MATLAB SCRIPT FOR SPRINGBACK OF FLEXURES

(Working file. May have been changed from original parameters)

```
clear all
Y=290*10^6; %yield strength
E=193*10^9; %youngs modulus
T=.0000762; %thickness (m)
Ri=.005; %initial radius
angle=15 %desired angle
format long
parenth=Ri*Y/(E*T);
bottom=4*parenth^3-3*parenth+1;
Rf=Ri/bottom  %final radius
s_arc=angle*2*pi*Rf/360 %arc length if final angle were 15 degrees
angle=360*s_arc/(2*pi*Ri) %initial angle

%results of note: if thickness .003" (.0000762m) and 15deg desired initial=21.18degrees
```

References

[1] H. Pohl, H.G. Welch, "The Role of Overdiagnosis and Reclassification in the Marked Increase of Esophageal Adenocarcinoma Incidence." J. Natl Cancer Inst, 2005, 97(2), pp 142-6.

[2] National Center for Health Statistics, "Ambulatory and Inpatient Procedures in the United States, 1996." Vital and Health Statistics, Series 13, No. 139, 1998.

[3] . McGrath PC, Sloan DA, Kenady DE. Surgical management of pancreatic carcinoma. Seminars in Oncology. 1996;23(2):200-12.

[4] Endosonography.dk, "Needle tip at the curved array transducer," http://www.endosonography.dk/EUS-siden/Atlas/7.57Tip.htm .

[5] Shung, Principles of Medical Imaging, p 85,Academic Press, 2003.

[6] Skarin, Atlas of Diagnostic Oncology, p18, 2003.

[7] William C. Culp, MD, Timothy C. McCowan, MD, Timothy C. Goertzen, MD, Thomas G. Habbe, MD, Michael M. Hummel, MD,Robert F. LeVeen, MD,Joseph C. Anderson, MD, *Relative Ultrasonographic Echogenicity of Standard, Dimpled, and Polymeric-coated Needles*, JVIR 2000; 11:351–358.

[8] Bockus, Gastroenterology 5th ed., Philadelphia, Sanders. p 397, 1995.

[9] Ilona M. Schmalfuss, MD, Anthony A. Mancuso, MD and Roger P. Tart, MD
Postcricoid Region and Cervical Esophagus: Normal Appearance at CT and MR Imaging. Radiology. 2000; 214:237-246.) © RSNA, 2000

[10] Grays Anatomy Online. 85 Hepatobiliary System: Liver

[11] Grays Anatomy Online. 88 Pancreas, Spleen and Suprarenal Gland

[12] Yamada, Strength of Biological Materials, Baltimore, Williams & Wilkins 1970

[11] Merriam Webster Dictionary (www.m-w.com)

[14] A.A. Bravo, S.G. Sheth, S.Chopra, "Liver biopsy." N Engl J Med, 344:495-500

[15] Hitachi, Model: FG-34UX, http://www.hitachi-medical-systems.com/us_probsys_probes.php?proId=4 .

[16] W.R. Brugge, Director GI Endoscopy Unit, Massachusetts General Hospital, *Personal Communication*. 2004.

[17] Cook Endoscopy, Model: EUSN-20-CPN, http://www.cookendoscopy.com/esoph/ultrasound/usn04.html.

[18] A.M. Okamura, C. Simone, M.D. O'Leary. "Force Modeling for Needle Insertion into Soft Tissue." IEEE Transactions on Biomedical Engineering, No. 10, Vol 51, Oct. 2004.

[19] A.A. Bravo, S.G. Sheth, S.Chopra, "Liver biopsy." N Engl J Med, 344:495-500

[20] Dr. William Brugge, Head of Gastroenterology, Massachusetts General Hospital. *Personal Communication*. 2005.

[21]E.A Avallone, Baumeister, T., III. Marks' Standard Handbook for Mechanical Engineers (10th Edition). P5-23. McGraw-Hill, 1996.

[22] J. Antony, Design of Experiments for Engineers and Scientists, Oxford, Butterworth-Heinemann, 2003.

[23] TA.XT Texture Analyzer, Texture Technologies Corp., Scarsdale, NY/Stable Micro Systems, Godalming, Surrey, UK.

[24] G. Mostovoy, Vaupell Rapid Solutions, *Personal Communication*. 2005.

[25] Budynas, Young, Roark's Formulas for Stress and Strain, 7th Edition, New York, McGraw Hill, 2002.

[26] PB Leiner, "Physical and Chemical Properties of Gelatin." www.gelatin.com .

[27] T.N. Erpelding, R.C. Booi, K.W. Hollman, M. O'Donnell, "Measuring Tissue Elastic Properties Using Acoustic Radiation Force on Laser-Generated Bubbles." IEEE Ultrasonics Symposium, 2003.

[28] H. Yamada, Strength of Biological Materials, Baltimore, Williams & Wilkins, 1970.

[29] Chanthasopeephan et. al, "Measuring Forces in Liver Cutting: New Equipment and Experimental Results." Annals of Biomedical Engineering, Vol 31, pp. 1372-1382, 2003.

[30] Chui, Kobayashi, Chen et. al, "Combined compression and elongation experiments and non-linear modeling of liver tissue for surgical simulation." Med. Biol. Eng. Comput., 42, 787-798, 2004.

[31] K.L. Johnson, Contact Mechanics, Cambridge University Press, 1985.

[32] Kraft Foods, www.kraftfoods.com/knox .

[33] PB Leiner, "Preparing Gelatin Solutions." www.gelatin.com .

[34] C. Simone, A.M. Okamura, "Modeling of Needle Insertion Forces for Robot-Assisted Percutaneous Therapy." IEEE International Conference on Robotics & Automation, pp. 2085-2091, 2002.

[35] Eagle Stainless Tube and Fabrication Inc., 10 Discovery Way, Franklin, MA 02038

[36] Kalpakjian, Schmid, Manufacturing Engineering and Technology, 5th Edition, New Jersey, Pearson Prentice Hall, 2006.

[37] Denise Gomez, Popper and Sons. *Personal Communication*. 2006.

[38] Chryssolouris, G. Laser machining : theory and practice, New York, Springer-Verlag, 1991.

[39] Eagle Stainless Tube and Fabrication Inc., 10 Discovery Way, Franklin, MA 02038